

# Island filters for partially observed spatiotemporal systems

Edward L. Ionides <sup>\*1</sup>, Kidus Asfaw<sup>1</sup>, Joonha Park<sup>2</sup>, and Aaron A. King<sup>3</sup>

<sup>1</sup>*Department of Statistics, University of Michigan*

<sup>2</sup>*Department of Mathematics and Statistics, Boston University*

<sup>3</sup>*Department of Ecology and Evolutionary Biology, Department of Mathematics, and Center for the Study of Complex Systems, University of Michigan*

June 11, 2022

## Abstract

Statistical inference for high-dimensional partially observed, nonlinear, stochastic processes is a methodological challenge with applications including spatiotemporal analysis of epidemiological and ecological systems. Standard particle filter algorithms, which provide an effective approach for general low-dimensional partially observed Markov processes, suffer from a curse of dimensionality that limits their applicability beyond low-dimensional systems. We show that many independent Monte Carlo calculations, none of which, by itself, attempts to solve the filtering problem, can be combined to give a global filtering solution that theoretically beats the curse of dimensionality under weak coupling conditions. The independent Monte Carlo calculations are called islands, and the corresponding algorithm is called a basic island filter (BIF). Carrying out an operation called adapted simulation on each island results in a variant called an adapted simulation island filter (ASIF). Adapted simulation can be implemented using a Monte Carlo technique called intermediate resampling to give the ASIF-IR algorithm which has improved theoretical and empirical scaling. Our focus is on evaluation of the likelihood function, but our algorithms and theory are also pertinent to latent state estimation. We demonstrate our methodology on coupled population dynamics arising in the epidemiology of infectious disease. In this context, our methods retain the generality of particle filter algorithms while scaling to systems an order of magnitude larger.

**Keywords:** Particle filter; sequential Monte Carlo; Markov process; spatiotemporal inference; metapopulation dynamics

---

<sup>\*</sup>To whom correspondence should be addressed. Email: ionides@umich.edu

## Introduction

Particle filter (PF) algorithms are a fundamental tool for inference on nonlinear partially observed dynamic systems (Doucet et al.; 2001; Doucet and Johansen; 2011; Bretó et al.; 2009; Ionides et al.; 2015). Standard PF methods suffer from a curse of dimensionality (COD), defined as an exponential increase in computational demands as the problem size grows Bengtsson et al. (2008); Snyder et al. (2015); Rebeschini and van Handel (2015). This limits the applicability of PF-based statistical methodology for high-dimensional systems which arise in spatiotemporal data analysis and other situations. In PF algorithms, particles are representations of latent variables. Groups of particles which have limited interaction within the algorithm are called *islands*. We say an *independent island particle filter* is a PF algorithm that constructs groups of non-interacting particles and then combines the results. The independence is understood in a Monte Carlo sense, with each island having access to the entire dataset. This geographic island metaphor describing the Monte Carlo computation is separate from any geographic structure that may, or may not, be present in a spatiotemporal model. A previous motivation for dividing particles into weakly interacting islands has been to minimize communication for parallelized PF algorithms (Vergé et al.; 2013; Del Moral et al.; 2017). We have a different motivation: to show that many independent PF calculations, each one of which is too weak to be useful by itself, can be combined to solve high-dimensional problems not amenable to solution by a single filter. Indeed, the calculation carried out on each island will not even attempt to directly solve the filtering problem. The task of each island is to provide a representation of the latent process that provides some relevant information at some points in space and time. The algorithms then proceed to combine these islands, assessing which islands are good representations at a given spatiotemporal location.

Independent island filters may be motivated by the empirical success of *poor man's ensemble* forecasting methodology in which a collection of independently constructed forecasts is generated using different models and methods (Ebert; 2001). Poor man's ensembles have sometimes been found to have greater forecasting skill than any one forecast (Leutbecher and Palmer; 2008; Palmer; 2002). One explanation for this phenomenon is that even a hypothetically perfect model cannot filter and forecast well using methodology afflicted by the COD. We show that independent island methodology can relieve this limitation. From this perspective, the independence of the forecasts in the poor man's ensemble, rather than the diversity of model structures, may be the key to its success.

Our idea is most clearly seen in a relatively simple algorithm which we call the basic island filter (BIF). Each island in BIF simply simulates a realization of the latent process model. While formally beating the COD under a weak mixing assumption, BIF could have poor numerical behavior if a very large number of islands were needed to reach this happy asymptotic limit. Our empirical results show that BIF may indeed be a useful algorithm in some situations, however it also provides a route toward two other algorithms which we call the adapted sampling island filter (ASIF) and adapted sampling island filter

with intermediate resampling (ASIF-IR). ASIF and ASIF-IR carry out some resampling on each island and therefore enable each island to track the data, in a weak sense, while resisting the COD.

## Notation

To set up notation, we suppose the latent process is comprised of a collection of units, labeled  $\{1, 2, \dots, U\}$  which we write as  $1:U$ . An unobserved, latent Markov process at a discrete sequence of observation times is written as  $\{\mathbf{X}_n, n \in 0:N\}$ , with  $\mathbf{X}_n = X_{1:U,n}$  taking values in  $\mathbb{X}^U$ . The initial value  $\mathbf{X}_0$  may be stochastic or deterministic. Observations are made on each unit, modeled by an observable process  $\{\mathbf{Y}_n = Y_{1:U,n}, n \in 1:N\}$  which takes values in  $\mathbb{Y}^U$ . Observations are modeled as being conditionally independent given the latent process. The conditional independence of measurements applies over both space and time, so  $Y_{u,n}$  is conditionally independent of  $Y_{\tilde{u},\tilde{n}}$  given  $X_{1:U,0:N}$  whenever  $(u, n) \neq (\tilde{u}, \tilde{n})$ . This unit structure for the observation process is not necessary for all that follows (see Sec. S1). We suppose the existence of a joint density  $f_{\mathbf{X}_{0:N}, \mathbf{Y}_{1:N}}$  of  $\{X_{1:U,n}\}$  and  $\{Y_{1:U,n}\}$  with respect to some appropriate measure. We use the same subscript notation to denote other marginal and conditional densities. The data are  $y_{u,n}$  for spatial unit  $u$  at time  $n$ . For a fixed value of  $U$ , this model fits into the partially observed Markov process (POMP) framework (Bretó et al.; 2009), also known as a state space model or hidden Markov model. Spatiotemporal POMP models are characterized by a high dimensionality, proportional to  $U$ , for the latent Markov process. We use the term SpatPOMP to describe POMP models indexed by  $u$  as well as  $n$ . In accordance with the spatial interpretation of the units  $u \in 1:U$ , we may suppose that units sufficiently distant in some sense approach independence, a phenomenon called *weak coupling*. Inference techniques for SpatPOMPs may be relevant to high-dimensional stochastic dynamic systems where  $u$  does not index spatial locations. The units will sometimes be considered in sequence within each time point, and so we write the set of points preceding  $(u, n)$  by

$$A_{u,n} = \{(\tilde{u}, \tilde{n}) : 1 \leq \tilde{n} < n \text{ or } (\tilde{n} = n \text{ and } \tilde{u} < u)\}. \quad (1)$$

An ordering of the spatial locations, required by [1], might seem artificial. Indeed, densities such as  $f_{X_{u,n}|X_{A_{u,n}}}$  could potentially be hard to compute or simulate from. The algorithms we study do not carry out such computations, but only evaluate the measurement model on these neighborhoods. To represent weak coupling, we suppose there is a neighborhood  $B_{u,n} \subset A_{u,n}$  such that the latent process on  $A_{u,n} \setminus B_{u,n}$  is approximately conditionally independent of  $X_{u,n}$  given data on  $B_{u,n}$ .

## Island filter methodology

The inputs for the BIF, ASIF and ASIF-IR are listed in Table 1. All three algorithms are *plug-and-play*, meaning that they require as input a simulator

for the latent dynamic process but not an evaluator of transition probabilities (Bretó et al.; 2009; He et al.; 2010). The primary output under consideration is an estimate of the log likelihood for the data given the model. The log likelihood  $\ell = \log f_{\mathbf{Y}_{1:N}}(\mathbf{y}_{1:N}^*)$  is a fundamental quantity for both Bayesian and non-Bayesian statistical inference. Monte Carlo estimates of the log likelihood underpin modern methods for full-information statistical inference on partially observed dynamic systems (Andrieu et al.; 2010; Ionides et al.; 2015, 2017). Filtering theory ties together the three tasks of likelihood evaluation, forecasting, and inferring latent dynamic variables Crisan and Rozovskii (2011). Successful likelihood evaluation is therefore closely related to success at forecasting and latent process reconstruction.

The pseudocodes for the algorithms that follow will adopt a convention that implicit loops are carried out over all free indices. For example, the construction of  $w_{u,n,i}^P$  in BIF has an implicit loop over  $u$ ,  $n$  and  $i$ . The construction of  $w_{u,n,i,j}^P$  in ASIF has an implicit loop over  $u$ ,  $i$  and  $j$  but not over  $n$  since  $n$  is already defined in an explicit loop and is therefore not a free index. Table 1 lists the ranges of the implicit loops for all following algorithms.

---

**Table 1. Island filter inputs, outputs and implicit loops.**

---

**input:**

simulator for  $f_{\mathbf{X}_0}(\mathbf{x}_0)$  and  $f_{\mathbf{X}_n|\mathbf{X}_{n-1}}(\mathbf{x}_n | \mathbf{x}_{n-1})$

evaluator for  $f_{Y_{u,n}|X_{u,n}}(y_{u,n} | x_{u,n})$

number of islands,  $\mathcal{I}$

neighborhood structure,  $B_{u,n}$

data,  $\mathbf{y}_{1:N}^*$

ASIF and ASIF-IR: particles per island,  $J$

ASIF-IR: number of intermediate timesteps,  $S$

ASIF-IR: measurement variance parameterizations,  $\overleftarrow{v}_{u,n}$  and  $\overrightarrow{v}_{u,n}$

ASIF-IR: approximate process and observation mean functions,  $\boldsymbol{\mu}$  and  $h_{u,n}$

**output:**

Log likelihood estimate,  $\ell^{\text{MC}} = \sum_{n=1}^N \sum_{u=1}^U \ell_{u,n}^{\text{MC}}$

**implicit loops:**

$u$  in  $1:U$ ,  $n$  in  $1:N$ ,  $i$  in  $1:\mathcal{I}$ ,  $j$  in  $1:J$

---

The BIF algorithm that follows amounts to an island filter with a single particle per island, with no weighting or resampling within each island.

---

**BIF. Basic island filter.**

---

Simulate  $\mathbf{X}_{0:N,i} \sim f_{\mathbf{X}_{0:N}}(\mathbf{x}_{0:N})$

Measurement weights,  $w_{u,n,i}^M = f_{Y_{u,n}|X_{u,n}}(y_{u,n}^* | X_{u,n,i})$

Prediction weights,  $w_{u,n,i}^P = \prod_{(\tilde{u}, \tilde{n}) \in B_{u,n}} w_{\tilde{u}, \tilde{n}, i}^M$

$\ell_{u,n}^{\text{MC}} = \log \left( \sum_{i=1}^{\mathcal{I}} w_{u,n,i}^M w_{u,n,i}^P \right) - \log \left( \sum_{i=1}^{\mathcal{I}} w_{u,n,i}^P \right)$

---

Theorem 1 shows that BIF can beat COD. However, an algorithm such as BIF, which doesn't carry out resampling, would require quick spatiotemporal

mixing for the simulated particles to remain relevant for predictions throughout a long time series. It may in practice be necessary to select simulations consistent with the data, much as standard PF algorithms do. We look for approaches that build on the basic insight of BIF while having superior practical performance.

Whereas the full global filtering problem may be intractable via importance sampling methods, a version of this problem local in space and time may nevertheless be feasible. Drawing a sample from the conditional density,  $f_{\mathbf{X}_n | \mathbf{Y}_n, \mathbf{X}_{n-1}}$ , is distinct from the filtering problem: we call this operation *adapted simulation*. For models where  $\mathbf{X}_n$  is close to  $\mathbf{X}_{n-1}$ , adapted simulation requires a local calculation that may be much easier than the full filtering calculation. The following adapted simulation island filter (ASIF) is constructed under a hypothesis that the adapted simulation problem is tractable. The adapted simulations are then reweighted in a neighborhood of each point in space and time to construct a local approximation to the filtering problem which leads to an estimate of the likelihood.

---

**ASIF. Adapted simulation island filter.**

---

Initialize adapted simulation:  $\mathbf{X}_{0,i}^A \sim f_{\mathbf{X}_0}(\mathbf{x}_0)$

For  $n$  in  $1:N$

Proposals:  $\mathbf{X}_{n,i,j}^P \sim f_{\mathbf{X}_n | X_{1:U,n-1}}(\mathbf{x}_n | \mathbf{X}_{n-1,i}^A)$

Measurement weights:  $w_{u,n,i,j}^M = f_{Y_{u,n} | X_{u,n}}(y_{u,n}^* | X_{u,n,i,j}^P)$

Adapted resampling weights:  $w_{n,i,j}^A = \prod_{u=1}^U w_{u,n,i,j}^M$

Resampling:  $\mathbb{P}[r(i) = a] = w_{n,i,a}^A \left( \sum_{k=1}^J w_{n,i,k}^A \right)^{-1}$

$\mathbf{X}_{n,i}^A = \mathbf{X}_{n,i,r(i)}^P$

$w_{u,n,i,j}^P = \prod_{\tilde{n}=1}^{n-1} \left[ \frac{1}{J} \sum_{k=1}^J \prod_{(\tilde{u}, \tilde{n}) \in B_{u,n}^{[\tilde{n}]}} w_{\tilde{u}, \tilde{n}, i, k}^M \right] \prod_{(\tilde{u}, n) \in B_{u,n}^{[n]}} w_{\tilde{u}, n, i, j}^M$

End for

$$\ell_{u,n}^{\text{MC}} = \log \left( \frac{\sum_{i=1}^{\mathcal{I}} \sum_{j=1}^J w_{u,n,i,j}^M w_{u,n,i,j}^P}{\sum_{i=1}^{\mathcal{I}} \sum_{j=1}^J w_{u,n,i,j}^P} \right)$$


---

In addition, we consider an algorithm which adds intermediate resampling to the adapted simulation islands, and is therefore termed ASIF-IR. Intermediate resampling involves assessing the satisfactory progress of particles toward the subsequent observation at a collection of times between observations. This is well defined when the latent system is a continuous time process  $\{\mathbf{X}(t)\}$  with observation times  $t_{1:N}$  such that  $\mathbf{X}_n = \mathbf{X}(t_n)$ . For a continuous time latent process model, intermediate resampling can have favorable scaling properties when the intermediate times

$$t_{n-1} = t_{n,0} < t_{n,1} < \dots < t_{n,S} = t_n$$

scale with  $S \approx U$  Park and Ionides (2019). In the case  $S = 1$ , ASIF-IR reduces to ASIF. Intermediate resampling was developed in the context of sequential Monte Carlo Del Moral and Murray (2015); Park and Ionides (2019); however,

the same theory and methodology can be applied to the simpler and easier problem of adapted simulation. ASIF-IR requires a guide function which assess the capability of each particle to explain future data. The implementation in this pseudocode constructs the guide  $g_{n,s,i,j}$  used by the guided intermediate resampling filter Park and Ionides (2019) which generalizes the popular auxiliary particle filter (Pitt and Shepard; 1999). The guide function affects numerical performance of the algorithm but not its correctness: it enables a computationally convenient approximation to improve performance on the intractable target problem. Our guide function supposes the availability of a deterministic function approximating evolution of the mean of the latent process, and uses simulations to assess variability around this mean. We write this as

$$\boldsymbol{\mu}(\boldsymbol{x}, s, t) \approx \mathbb{E}[\boldsymbol{X}(t) \mid \boldsymbol{X}(s) = \boldsymbol{x}].$$

Further, the guide requires that the measurement model has known conditional mean and variance as a function of the model parameter vector  $\boldsymbol{\theta}$ , written as

$$\begin{aligned} h_{u,n}(x_{u,n}) &= \mathbb{E}[Y_{u,n} \mid X_{u,n} = x_{u,n}] \\ \vec{v}_{u,n}(x_{u,n}, \boldsymbol{\theta}) &= \text{Var}(Y_{u,n} \mid X_{u,n} = x_{u,n}; \boldsymbol{\theta}) \end{aligned}$$

Also required for ASIF-IR is an inverse function  $\overleftarrow{v}_{u,n}$  such that

$$\vec{v}_{u,n}(x_{u,n}, \overleftarrow{v}_{u,n}(V, x_{u,n}, \boldsymbol{\theta})) = V.$$

This guide function is applicable to spatiotemporal versions of a broad range of population and compartment models used to model dynamic systems in ecology, epidemiology, and elsewhere. Other guide functions could be developed and inserted into the ASIF-IR algorithm. The number of particles for the guide simulations in ASIF-IR does not necessarily have to be set equal to the number of intermediate proposals. We make that simplification here since there is no compelling reason against it.

---

**ASIF-IR. Adapted simulation island filter with  
intermediate resampling.**

---

Initialize adapted simulation:  $\mathbf{X}_{0,i}^A \sim f_{\mathbf{X}_0}(\mathbf{x}_0)$

For  $n$  in 1: $N$

Guide simulations:  $\mathbf{X}_{n,i,j}^G \sim f_{\mathbf{X}_n|\mathbf{X}_{n-1}}(\mathbf{x}_n | \mathbf{X}_{n-1,i}^A)$

Guide variance:  $V_{u,n,i} = \text{Var}\{h_{u,n}(X_{u,n,i,j}^G), j \text{ in } 1:J\}$

$g_{n,0,i,j}^R = 1$  and  $\mathbf{X}_{n,0,i,j}^{\text{IR}} = \mathbf{X}_{n-1,i}^A$

For  $s$  in 1: $S$

Intermediate proposals:  $\mathbf{X}_{n,s,i,j}^{\text{IP}} \sim f_{\mathbf{X}_{n,s}|\mathbf{X}_{n,s-1}}(\cdot | \mathbf{X}_{n,s-1,i,j}^{\text{IR}})$

$\boldsymbol{\mu}_{n,s,i,j}^{\text{IP}} = \boldsymbol{\mu}(\mathbf{X}_{n,s,i,j}^{\text{IP}}, t_{n,s}, t_n)$

$V_{u,n,s,i,j}^{\text{meas}} = \vec{v}_u(\theta, \boldsymbol{\mu}_{u,n,s,i,j}^{\text{IP}})$

$V_{u,n,s,i}^{\text{proc}} = V_{u,n,i}(t_n - t_{n,s}) / (t_n - t_{n,0})$

$\theta_{u,n,s,i,j} = \vec{v}_u(V_{u,n,s,i,j}^{\text{meas}} + V_{u,n,s,i}^{\text{proc}}, \boldsymbol{\mu}_{u,n,s,i,j}^{\text{IP}})$

$g_{n,s,i,j} = \prod_{u=1}^U f_{Y_{u,n}|X_{u,n}}(y_{u,n}^* | \boldsymbol{\mu}_{u,n,s,i,j}^{\text{IP}}; \theta_{u,n,s,i,j})$

Guide weights:  $w_{n,s,i,j}^G = g_{n,s,i,j} / g_{n,s-1,i,j}^R$

Resampling:  $\mathbb{P}[r(i,j) = a] = w_{n,s,i,a}^G \left( \sum_{k=1}^J w_{n,s,i,k}^G \right)^{-1}$

$\mathbf{X}_{n,s,i,j}^{\text{IR}} = \mathbf{X}_{n,s,i,r(i,j)}^{\text{IP}}$  and  $g_{n,s,i,j}^R = g_{n,s,i,r(i,j)}$

End For

Set  $\mathbf{X}_{n,i}^A = \mathbf{X}_{n,S,i,1}^{\text{IR}}$

Measurement weights:  $w_{u,n,i,j}^M = f_{Y_{u,n}|X_{u,n}}(y_{u,n}^* | X_{u,n,i,j}^G)$

$$w_{u,n,i,j}^P = \prod_{\tilde{n}=1}^{n-1} \left[ \frac{1}{J} \sum_{a=1}^J \prod_{(\tilde{u}, \tilde{n}) \in B_{u,\tilde{n}}^{[\tilde{n}]}} w_{\tilde{u}, \tilde{n}, i, a}^M \right] \prod_{(\tilde{u}, n) \in B_{u,n}^{[n]}} w_{\tilde{u}, n, i, j}^M$$

End for

$$\ell_{u,n}^{\text{MC}} = \log \left( \frac{\sum_{i=1}^{\mathcal{I}} \sum_{j=1}^J w_{u,n,i,j}^M w_{u,n,i,j}^P}{\sum_{i=1}^{\mathcal{I}} \sum_{j=1}^J w_{u,n,i,j}^P} \right)$$


---

One might wonder why it is appropriate to keep many particle representations at intermediate timesteps while resampling down to a single representative at each observation time. Part of the answer is that adaptive simulation can fail in a limit with high frequency observations (Sec. S2). This implies that adapted simulation should not be relied upon more than necessary to ameliorate the curse of dimensionality: once proper importance sampling for filtering problem becomes tractable in a sufficiently small spatiotemporal neighborhood, one should maintain weighted particles on this spatiotemporal scale rather than resorting to adapted simulation.

## Likelihood factorizations and their approximations

The approximation error for the algorithms we study here can be divided into two sources: a localization bias due to conditioning on a finite neighborhood, and Monte Carlo error. The localization bias does not disappear in the limit as

Monte Carlo effort increases. It does become small as the conditioning neighborhood increases, but the Monte Carlo effort grows exponentially in the size of this neighborhood. The class of problems for which these algorithms are useful are ones where a relatively small neighborhood is adequate. Although the filtering inference is carried out using localization, the simulation of the process is carried out globally which avoids the introduction of additional boundary effects and ensures that the simulations comply with any constraint properties of the global process simulator.

In this subsection, we consider the deterministic limit of each algorithm for infinite Monte Carlo effort. We explain why the BIF, ASIF and ASIF-IR algorithms approximately target the likelihood function, subject to suitable mixing behavior. Subsequently, we consider the scaling properties as Monte Carlo effort increases. We adopt a convention that densities involving  $Y_{u,n}$  are implicitly evaluated at the data,  $y_{u,n}^*$ , and densities involving  $X_{u,n}$  are implicitly evaluated at  $x_{u,n}$  unless otherwise specified. We write  $A_{u,n}^+ = A_{u,n} \cup (u, n)$  and  $B_{u,n}^+ = B_{u,n} \cup (u, n)$ . All the algorithms localize the sequential factorization of the likelihood,

$$f_{Y_{1:U}, 1:N} = \prod_{n=1}^N \prod_{u=1}^U f_{Y_{u,n} | Y_{A_{u,n}}} = \prod_{n=1}^N \prod_{u=1}^U \frac{f_{Y_{A_{u,n}^+}}}{f_{Y_{A_{u,n}}}},$$

by employing approximations that assume a neighborhood  $B_{u,n} \subset A_{u,n}$  is sufficient in place of the full history  $A_{u,n}$ . BIF approximates  $f_{Y_{u,n} | Y_{A_{u,n}}}$  by

$$f_{Y_{u,n} | Y_{B_{u,n}}} = \frac{f_{Y_{B_{u,n}^+}}}{f_{Y_{B_{u,n}}}} = \frac{\int f_{Y_{B_{u,n}^+} | X_{B_{u,n}^+}} f_{X_{B_{u,n}^+}} dx_{B_{u,n}^+}}{\int f_{Y_{B_{u,n}} | X_{B_{u,n}}} f_{X_{B_{u,n}}} dx_{B_{u,n}}}.$$

For  $B \subset 1:U \times 1:N$ , define  $B^{[m]} = B \cap (1:U \times \{m\})$ . ASIF and ASIF-IR build on the following identity,

$$f_{Y_{A_{u,n}}} = \int f_{\mathbf{X}_0} \left[ \prod_{m=1}^n f_{\mathbf{X}_m | \mathbf{X}_{m-1}, \mathbf{Y}_m} f_{Y_{A_{u,n}^{[m]} | \mathbf{X}_{m-1}}} \right] d\mathbf{x}_{0:n},$$

where  $f_{\mathbf{X}_m | \mathbf{X}_{m-1}, \mathbf{Y}_m}$  is called the adapted transition density. The adapted process (i.e., a stochastic process following the adapted transition density) can be interpreted as a one-step greedy procedure using the data to guide the latent process. Let  $g_{\mathbf{X}_{0:N}, \mathbf{X}_{1:N}^P}(\mathbf{x}_{0:N}, \mathbf{x}_{1:N}^P)$  be the joint density of the adapted process and the proposal process,

$$g_{\mathbf{X}_{0:N}, \mathbf{X}_{1:N}^P}(\mathbf{x}_{0:N}, \mathbf{x}_{1:N}^P) = f_{\mathbf{X}_0}(\mathbf{x}_0) \times \prod_{n=1}^N f_{\mathbf{X}_n | \mathbf{X}_{n-1}, \mathbf{Y}_n}(\mathbf{x}_n | \mathbf{x}_{n-1}, \mathbf{y}_n^*) f_{\mathbf{X}_n | \mathbf{X}_{n-1}}(\mathbf{x}_n^P | \mathbf{x}_{n-1}). \quad (2)$$



For  $B \subset 1:U \times 1:N$ , define  $B^{[m]} = B \cap (1:U \times \{m\})$  and set

$$\gamma_B = \prod_{m=1}^N f_{Y_{B^{[m]}|\mathbf{X}_{m-1}}}(y_{B^{[m]}}^* | \mathbf{X}_{m-1}),$$

using the convention that an empty density  $f_{Y_\emptyset}$  evaluates to 1. Denoting  $\mathbb{E}_g$  for expectation for  $(\mathbf{X}_{0:N}, \mathbf{X}_{1:N}^P)$  having density  $g_{\mathbf{X}_{0:N}, \mathbf{X}_{1:N}^P}$ , we have

$$f_{Y_{u,n}|Y_{A_{u,n}}} = \frac{\mathbb{E}_{g_n}[\gamma_{A_{u,n}^+}]}{\mathbb{E}_{g_n}[\gamma_{A_{u,n}}]}.$$

Estimating this ratio by Monte Carlo sampling from  $g_n$  is problematic due to the growing size of  $A_{u,n}$ . Thus, ASIF and ASIF-IR make a localized approximation,

$$\frac{\mathbb{E}_{g_n}[\gamma_{A_{u,n}^+}]}{\mathbb{E}_{g_n}[\gamma_{A_{u,n}}]} \approx \frac{\mathbb{E}_{g_n}[\gamma_{B_{u,n}^+}]}{\mathbb{E}_{g_n}[\gamma_{B_{u,n}}]}. \quad (3)$$

The conditional log likelihood estimate  $\ell_{u,n}^{\text{MC}}$  in ASIF and ASIF-IR come from replacing the expectations on the right hand side of [3] with averages over Monte Carlo replicates of simulations from the adapted process. To see that we expect the approximation in [3] to hold when dependence decays across spatiotemporal distance, we can write

$$\begin{aligned} \gamma_{A_{u,n}} &= \gamma_{B_{u,n}} \gamma_{B_{u,n}^c} \\ \gamma_{A_{u,n}^+} &= \gamma_{B_{u,n}^+} \gamma_{B_{u,n}^c}, \end{aligned}$$

where  $B_{u,n}^c$  is the complement of  $B_{u,n}$  in  $A_{u,n}$ . As long as  $\gamma_{B_{u,n}^c}$  is approximately independent of  $X_{u,n}$  under  $g_n$ , this term approximately cancels in the numerator and denominator of the right hand side of [3].

## BIF theory

For each pair  $(U, N)$  we suppose there is a dataset  $\mathbf{y}_{1:N}^*$  and a model  $f_{\mathbf{X}_{0:N}, \mathbf{Y}_{1:N}}$ . We are interested in results that hold for all  $(U, N)$ , but we do not require that the models for  $(U_1, N_1) \neq (U_2, N_2)$  are nested in any way. The following conditions impose requirements that distant regions of space-time behave similarly and have only weak dependence. The conditions are written non-asymptotically in terms of  $\epsilon > 0$  and  $Q > 1$  which are used to bound the asymptotic bias and variance in Theorem 1. Stronger bounds are obtained when the conditions hold for small  $\epsilon_{A1}$ ,  $\epsilon_{A4}$  and  $Q$ .

**Assumption A1.** *There is an  $\epsilon_{A1} > 0$  and a collection of neighborhoods  $\{B_{u,n} \subset A_{u,n}, u \in 1:U, n \in 1:N\}$  such that, for all  $u, n, U, N$ , any bounded*

real-valued function  $|h(x)| \leq 1$ , and any value of  $x_{B_{u,n}^c}$ ,

$$\left| \int h(x_{u,n}) f_{X_{u,n}|Y_{B_{u,n}}, X_{B_{u,n}^c}}(x_{u,n} | y_{B_{u,n}}^*, x_{B_{u,n}^c}) dx_{u,n} - \int h(x_{u,n}) f_{X_{u,n}|Y_{B_{u,n}}}(x_{u,n} | y_{B_{u,n}}^*) dx_{u,n} \right| < \epsilon_{A1}.$$

**Assumption A2.** For the collection of neighborhoods in Assumption A1, with  $B_{u,n}^+ = B_{u,n} \cup (u, n)$ , there is a constant  $b$ , depending on  $\epsilon_{A1}$  but not on  $U$  and  $N$ , such that

$$\sup_{u \in 1:U, n \in 1:N} |B_{u,n}^+| \leq b.$$

**Assumption A3.** There is a constant  $Q$  such that, for all  $u$  and  $n$ ,  $U$  and  $N$ ,

$$Q^{-1} < f_{Y_{u,n}|X_{u,n}}(y_{u,n}^* | x_{u,n}) < Q$$

**Assumption A4.** There exists  $\epsilon_{A4} > 0$  such that the following holds. For each  $u, n$ , a set  $C_{u,n} \subset (1:U) \times (0:N)$  exists such that  $(\tilde{u}, \tilde{n}) \notin C_{u,n}$  implies  $B_{u,n}^+ \cap B_{\tilde{u},\tilde{n}}^+ = \emptyset$  and

$$|f_{X_{B_{\tilde{u},\tilde{n}}^+}|X_{B_{u,n}^+}} - f_{X_{B_{u,n}^+}}| < \epsilon_{A4} f_{X_{B_{\tilde{u},\tilde{n}}^+}}$$

Further, there is a uniform bound  $|C_{u,n}| \leq c$ .

The two mixing conditions in Assumptions A1 and A4 are subtly different. Assumption A1 is a conditional mixing property, dependent on the data, whereas A4 asserts a form of unconditional mixing. Although both capture a similar concept of weak coupling, conditional and unconditional mixing properties do not readily imply one another. Assumption A3 is a compactness condition of a type that has proved useful in the theory of particle filters despite the rarity of its holding exactly. Theorem 1 shows that these conditions let BIF compute the likelihood with a Monte Carlo variance of order  $UN\mathcal{I}^{-1}$  with a bias of order  $UN\epsilon$ .

**Theorem 1.** Let  $\ell^{MC}$  denote the Monte Carlo likelihood approximation constructed by BIF. Consider a limit with a growing number of islands,  $\mathcal{I} \rightarrow \infty$ , and suppose assumptions A1, A2 and A3. There are quantities  $\epsilon(U, N)$  and  $V(U, N)$ , with bounds  $|\epsilon| < \epsilon_{A1} Q^2$  and  $V < Q^{4b} U^2 N^2$ , such that

$$\mathcal{I}^{1/2} [\ell^{MC} - \ell - \epsilon UN] \xrightarrow[\mathcal{I} \rightarrow \infty]{d} \mathcal{N}[0, V], \quad (4)$$

where  $\xrightarrow[\mathcal{I} \rightarrow \infty]{d}$  denotes convergence in distribution and  $\mathcal{N}[\mu, \Sigma]$  is the normal distribution with mean  $\mu$  and variance  $\Sigma$ . If additionally Assumption A4 holds, we obtain an improved variance bound

$$V < Q^{4b} UN(c + \epsilon_{A4}(UN - c)). \quad (5)$$

*Proof.* A complete proof is given in Sec. S3. Briefly, the assumptions imply a multivariate central limit theorem for  $\{\ell_{u,n}^{\text{MC}}, (u, n) \in 1:U \times 1:N\}$  as  $\mathcal{I} \rightarrow \infty$ . The limiting variances and covariances are uniformly bounded, using Assumptions A2 and A3. Assumption A1 provides a uniform bound on the discrepancy between  $\ell_{u,n}$  and mean of the Gaussian limit. This is enough to derive [4]. Assumption A4 gives a stronger bound on covariances between sufficiently distant units, leading to [5].  $\square$

## ASIF-IR theory

Since ASIF is ASIF-IR with  $S = 1$ , we focus attention on ASIF-IR. At a conceptual level, the localized likelihood estimate in ASIF-IR has the same structure as its BIF counterpart. However, ASIF-IR additionally requires the capability to satisfactorily implement adapted simulation. Adapted simulation is a local calculation, making it an easier task than the global operation of filtering. Nevertheless, adapted simulation via importance sampling is vulnerable to COD for sufficiently large values of  $U$ . For a continuous time model, the use of  $S > 1$  is motivated by a result that guided intermediate resampling can reduce, or even remove, the COD in the context of a particle filtering algorithm Park and Ionides (2019). Assumptions B1–B4 are analogous to A1–A4 and are non-asymptotic assumptions involving  $\epsilon_{\text{B1}} > 0$ ,  $\epsilon_{\text{B4}} > 0$  and  $Q > 1$  which are required to hold uniformly over space and time. Assumption B5–B7 control the Monte Carlo error arising from adapted simulation. B5 is a stability property which ensures the Monte Carlo error cannot grow with time. Assumption B6 is a non-asymptotic bound on Monte Carlo error for a single step of adapted simulation. Assumption B7 can be guaranteed by the construction of the algorithm, if independently generated Monte Carlo random variables are used for building the guide function and the one-step prediction particles. The asymptotic limit in Theorem 2 arises as the number of islands increases.

**Assumption B1.** *There is an  $\epsilon_{\text{B1}} > 0$  and a collection of neighborhoods  $\{B_{u,n} \subset A_{u,n}, u \in 1:U, n \in 1:N\}$  such that the following holds for all  $u, n, U, N$ , and any bounded real-valued function  $|h(x)| \leq 1$ : if we write  $A = A_{u,n}$ ,  $B = B_{u,n}$ ,  $f_A(x_A) = f_{Y_A|X_A}(y_A^*|x_A)$ , and  $f_B(x_B) = f_{Y_B|X_B}(y_B^*|x_B)$ ,*

$$\left| \int h(x) \left\{ \frac{\mathbb{E}_g[f_A(X_A^P) f_{X_{u,n}|X_{A[n]}, \mathbf{X}_{n-1}}(x|X_{A[n]}^P, \mathbf{X}_{n-1})]}{\mathbb{E}_g[f_A(X_A^P)]} - \frac{\mathbb{E}_g[f_B(X_B^P) f_{X_{u,n}|X_{B[n]}, \mathbf{X}_{n-1}}(x|X_{B[n]}^P, \mathbf{X}_{n-1})]}{\mathbb{E}_g[f_B(X_B^P)]} \right\} dx \right| < \epsilon_{\text{B1}}.$$

**Assumption B2.** *The bound  $\sup_{u \in 1:U, n \in 1:N} |B_{u,n}^+| \leq b$  in Assumption A2 applies for the neighborhoods defined in Assumption B1. This also implies there is a finite maximum temporal depth for the collection of neighborhoods, defined as*

$$d_{\text{max}} = \sup_{(u,n)} \sup_{(\tilde{u}, \tilde{n}) \in B_{u,n}} |n - \tilde{n}|.$$

**Assumption B3.** Identically to Assumption A3,  $Q^{-1} < f_{Y_{u,n}|X_{u,n}}(g_{u,n}^* | x_{u,n}) < Q$ .

**Assumption B4.** Define  $g_{X_A|X_B}$  via [2]. Suppose there is an  $\epsilon_{B4}$  such that the following holds. For each  $u, n$ , a set  $C_{u,n} \subset (1:U) \times (0:N)$  exists such that  $(\tilde{u}, \tilde{n}) \notin C_{u,n}$  implies  $B_{u,n}^+ \cap B_{\tilde{u},\tilde{n}}^+ = \emptyset$  and

$$\begin{aligned} & \left| g_{X_{B_{\tilde{u},\tilde{n}}}^P | X_{B_{u,n}}^P} - g_{X_{B_{\tilde{u},\tilde{n}}}^P | X_{B_{u,n}}^P} \right| < (1/2) \epsilon_{B4} g_{X_{B_{\tilde{u},\tilde{n}}}^P} g_{X_{B_{u,n}}^P} \\ & \left| g_{X_{B_{\tilde{u},\tilde{n}}}^P | \mathbf{X}_{0:N}} g_{X_{B_{u,n}}^P | \mathbf{X}_{0:N}} - g_{X_{B_{\tilde{u},\tilde{n}}}^P, X_{B_{u,n}}^P | \mathbf{X}_{0:N}} \right| \\ & < (1/2) \epsilon_{B4} g_{X_{B_{\tilde{u},\tilde{n}}}^P, X_{B_{u,n}}^P | \mathbf{X}_{0:N}} \end{aligned}$$

Further, there is a uniform bound  $|C_{u,n}| \leq c$ .

**Assumption B5.** There is a constant  $K$  such that, for any set  $D \subset (1:U) \times (n:n-d)$  and for all  $n \geq K+d$ ,  $\mathbf{x}_{n-d-K}^{(1)}$ ,  $\mathbf{x}_{n-d-K}^{(2)}$ , and all  $x_{D_n}$ ,

$$\begin{aligned} & \left| g_{X_D | \mathbf{X}_{n-d-K}}(x_D | \mathbf{x}_{n-d-K}^{(1)}) - g_{X_D | \mathbf{X}_{n-d-K}}(x_D | \mathbf{x}_{n-d-K}^{(2)}) \right| \\ & < \epsilon_{B5} g_{X_D | \mathbf{X}_{n-d-K}}(x_{D_n} | \mathbf{x}_{n-d-K}^{(1)}) \end{aligned}$$

**Assumption B6.** Let  $h$  be a bounded function with  $|h(x)| \leq 1$ . Let  $\mathbf{X}_{n,S,j,i}^{\text{IR}}$  be the Monte Carlo quantity constructed in ASIF-IR, conditional on  $\mathbf{X}_{n-1,S,i}^A = \mathbf{x}_{n-1,S,i}^A$ . There is a constant  $C_0(U, N, S)$  such that, for all  $\epsilon_{B6} > 0$  and  $\mathbf{x}_{n-1,S,i}^A$ , whenever the number of particles satisfies  $J > C_0(U, N, S)/\epsilon_{B6}^4$ ,

$$\left| \mathbb{E} \left[ \frac{1}{J} \sum_{j=1}^J h(\mathbf{X}_{n,S,j,i}^{\text{IR}}) \right] - \mathbb{E}_g[h(\mathbf{X}_n) | \mathbf{X}_{n-1} = \mathbf{x}_{n-1,S,i}^A] \right| < \epsilon_{B6}.$$

**Assumption B7.** For  $1 \leq n \leq N$ , the Monte Carlo random variable  $X_{n,i}^A$  is independent of  $w_{u,n,i,j}^M$  conditional on  $X_{n-1,i}^A$ .

**Theorem 2.** Let  $\ell^{\text{MC}}$  denote the Monte Carlo likelihood approximation constructed by ASIF-IR, or by ASIF since this is the special case of ASIF-IR with  $S = 1$ . Consider a limit with a growing number of islands,  $\mathcal{I} \rightarrow \infty$ , and suppose assumptions B1, B2, B3, B5, B6 and B7. Suppose the number of particles  $J$  exceeds the requirement for B6. There are quantities  $\epsilon(U, N)$  and  $V(U, N)$  with  $|\epsilon| < Q^2 \epsilon_{B1} + 2Q^{2b}(\epsilon_{B5} + (K + d_{u,n})\epsilon_{B6})$  and  $V < Q^{4b}U^2N^2$  such that

$$\mathcal{I}^{1/2}[\ell^{\text{MC}} - \ell - \epsilon UN] \xrightarrow{\mathcal{I} \rightarrow \infty} \mathcal{N}[0, V].$$

If additionally Assumption B4 holds, we obtain an improved rate of

$$V < Q^{4b}NU \{c + (\epsilon_{B4} + 3\epsilon_{B5} + 4(K + d_{\max})\epsilon_{B6})(NU - c)\}$$

*Proof.* A full proof is provided in Sec. S4. The extra work to prove Theorem 2 beyond the argument for Theorem 1 is to bound the error arising from the importance sampling approximation to a draw from the adapted transition density. This bound is constructed using Assumptions B5, B6 and B7. The scaling of the constant  $\mathcal{C}_0$  with  $U$ ,  $N$  and  $S$  in Assumption B6 has been studied by Park and Ionides (2019), where it was established that setting  $S = U$  can lead to  $\mathcal{C}_0$  being constant or slowly growing with  $U$ . The remainder of the proof follows the same approach as Theorem 1, with the adapted process replacing the unconditional latent process.  $\square$

The theoretical results foreshadow our empirical observations that the relative performance of BIF, ASIF and ASIF-IR is situation-dependent. Assumption A4 is a mixing assumption for the unconditional latent process, whereas Assumption B4 replaces this with a mixing assumption for the adapted process conditional on the data. For a non-stationary process, Assumption A4 may fail to hold uniformly in  $U$  whereas the adapted process may provide stable tracking of the latent process (Sec. S2). When Assumption A4 is satisfactory, BIF can benefit from not requiring Assumptions B5, B6 and B7. Adapted simulation is an easier problem than filtering, but nevertheless can become difficult in high dimensions, with the consequence that Assumption B6 could require large  $\mathcal{C}_0$ . The tradeoff between ASIF and ASIF-IR depends on the effectiveness of the guide function for the problem at hand. Intermediate resampling and guide function calculation require additional computational resources, which will necessitate smaller values of  $\mathcal{I}$  and  $J$ . In some situations, the improved scaling properties of ASIF-IR compared to ASIF, corresponding to a lower value of  $\mathcal{C}_0$ , will outweigh this cost.

## Examples

Likelihood evaluation via filtering does not by itself enable parameter estimation for POMP models, however it provides a foundation for Bayesian Andrieu et al. (2010) and likelihood-based Ionides et al. (2015) inference. We therefore investigate likelihood evaluation with the expectation that improved methods for likelihood evaluation will lead to improved statistical methodology. Monte Carlo methods for computing the log likelihood generally suffer from both bias and variance, both of which can be considerable for large datasets and complex models. Appropriate inference methodology, such as Monte Carlo adjusted profile (MCAP) confidence intervals, can accommodate substantial Monte Carlo variance so long as the bias is slowly varying across the statistically plausible region of the parameter space Ionides et al. (2017).

We first compare the performance of the three island filters (BIF, ASIF and ASIF-IR) and alternative approaches, on a spatiotemporal Gaussian process for which the exact likelihood is available via a Kalman filter. We see in Fig. 1 that ASIF-IR can have a considerable advantages over BIF and ASIF for problems with an intermediate level of coupling. We then develop a model for measles

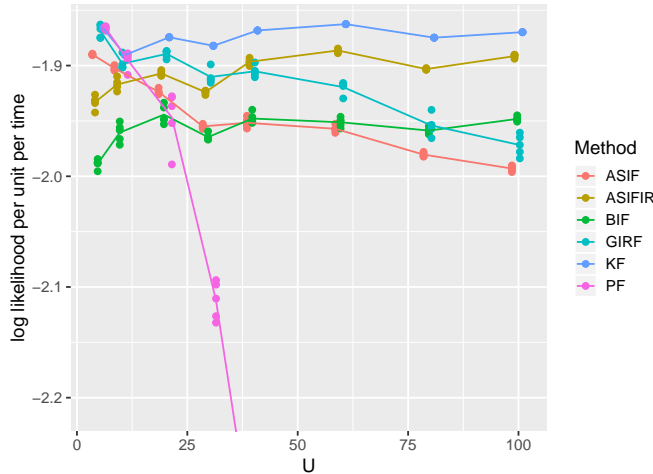


Figure 1: log likelihood estimates for a correlated Brownian motion model of various dimensions. BIF, ASIF and ASIF-IR are compared with a guided intermediate resampling filter (GIRF) and basic particle filter (PF). The exact likelihood was computed via a Kalman filter (KF).

transmission within and between cities. The model is weakly coupled, leading to successful performance for all three island filters. This class of metapopulation models was the primary motivation for the development of these methodologies. However, for a highly coupled system of moderate dimensions, a global particle filter such as GIRF may outperform our island methods; an example is given in Sec. S9.

## Correlated Brownian motion

Suppose  $\mathbf{X}(t) = \Omega \mathbf{W}(t)$  where  $\mathbf{W}(t) = W_{1:U}(t)$  comprises  $U$  independent standard Brownian motions, and  $\Omega_{u,\tilde{u}} = \rho^{d(u,\tilde{u})}$  with  $d(u,\tilde{u})$  being the circle distance,

$$d(u,\tilde{u}) = \min(|u - \tilde{u}|, |u - \tilde{u} + U|, |u - \tilde{u} - U|).$$

Set  $t_n = n$  for  $n = 0, 1, \dots, N$  with initial value  $\mathbf{X}(0) = \mathbf{0}$  and suppose measurement errors are independent and normally distributed,  $Y_{u,n} = X_{u,n} + \eta_{u,n}$  with  $\eta_{u,n} \sim \mathcal{N}(0, \tau^2)$ . The parameter  $\rho$  determines the strength of the spatial coupling.

Fig. 1 shows how the Monte Carlo error of the island filters compares to a standard particle filter (PF) and a guided intermediate resampling filter (GIRF) Park and Ionides (2019). For our numerical results, we use  $\tau = 1$ ,  $\rho = 0.4$  and  $N = 50$ . The algorithmic parameters and run times are listed in Sec. S5, together with a plot of the simulated data and supplementary discussion. The GIRF framework encompasses lookahead particle filter techniques, such as the

auxiliary particle filter Pitt and Shepard (1999), and intermediate resampling techniques Del Moral et al. (2017). GIRF methods combining these techniques were found to perform better than either of these component techniques alone Park and Ionides (2019). Thus, GIRF here represents a state-of-the-art auxiliary particle filter that targets the complete joint filter density for all units. We use the general-purpose, plug-and-play implementation of GIRF provided by the `spatPomp` R package (Asfaw et al.; 2019); this implementation of GIRF is thus not tailored in any way to exploit special features of this toy model. The true log likelihood can be computed analytically via the Kalman Filter (KF) in this simple Gaussian case. PF works well for small values of  $U$  in Fig. 1, but rapidly starts struggling as  $U$  increases. GIRF behaves comparably to PF for small  $U$  but its performance is maintained for larger  $U$ . ASIF and ASIF-IR have a small efficiency loss, for small  $U$ , relative to PF due to the localization involved in the filter weighting, but for large  $U$  this cost is more than paid back by the benefit of the reduced Monte Carlo variability. BIF has a larger efficiency loss for small  $U$ , but its favorable scaling properties lead it to overtake all but ASIF-IR for larger  $U$ . This linear Gaussian SpatPOMP model provides a simple scenario to demonstrate scaling behavior. We now move on to a more complex SpatPOMP exemplifying the nonlinear models motivating our new filtering approach.

## Spatiotemporal measles epidemics

Data analysis for spatiotemporal systems featuring nonlinear, nonstationary mechanisms and partial observability has been a longstanding open challenge for ecological and epidemiological analysis Bjørnstad and Grenfell (2001). A compartment modeling framework for spatiotemporal population dynamics divides the population at each spatial location into categories (called compartments) which are modeled as homogeneous. Spatiotemporal compartment models can be called patch models or metapopulation models in an ecological context. Particle filter methods based on targeted proposal distributions have been developed for spatiotemporal applications, but such methods suffer from the curse of dimensionality Snyder et al. (2015). The ensemble Kalman filter provides a state-of-the-art approach to high-dimensional spatiotemporal filtering, but the approximations inherent in the EnKF can be problematic for models that are highly nonlinear or non-Gaussian Ades and Van Leeuwen (2015). Our island filter methodologies have theoretical guarantees for arbitrarily nonlinear and non-Gaussian models, while having improved scaling properties compared to particle filters.

We consider a spatiotemporal model for disease transmission dynamics of measles within and between multiple cities, based on the model of Park and Ionides (2019) which adds spatial interaction to the compartment model presented by He et al. (2010). The model compartmentalizes the population of each city into susceptible ( $S$ ), exposed ( $E$ ), infectious ( $I$ ), and recovered/removed ( $R$ ) categories. The number of individuals in each compartment city  $u$  at time  $t$  are denoted by  $S_u(t)$ ,  $E_u(t)$ ,  $I_u(t)$ , and  $R_u(t)$ . The population dynamics are written in terms of non-decreasing processes  $N_{\bullet\bullet,u}(t)$  counting the cumulative

transitions in city  $u$ , up to time  $t$ , between compartments identified by the subscripts. Our model is described by the following system of stochastic differential equations, for  $u = 1, \dots, U$ ,

$$\begin{aligned} dS_u(t) &= dN_{BS,u}(t) - dN_{SE,u}(t) - dN_{SD,u}(t) \\ dE_u(t) &= dN_{SE,u}(t) - dN_{EI,u}(t) - dN_{ED,u}(t) \\ dI_u(t) &= dN_{EI,u}(t) - dN_{IR,u}(t) - dN_{ID,u}(t) \end{aligned}$$

Here,  $N_{BS,u}(t)$  models recruitment into the susceptible population, and  $N_{\bullet D,u}(t)$  models emigration and death. When  $N_{\bullet\bullet,u}(t)$  is integer-valued, the system has step function solutions. The total population  $P_u(t) = S_u(t) + E_u(t) + I_u(t) + R_u(t)$  is calculated by smoothing census data and is treated as known. The number of recovered individuals  $R_u(t)$  in city  $u$  is therefore defined implicitly.  $N_{SE,u}(t)$  is modeled as negative binomial death processes Bretó et al. (2009); Bretó and Ionides (2011) with over-dispersion parameter  $\sigma_{SE}$ , and rate given by

$$\begin{aligned} \mathbb{E}[N_{SE,u}(t+dt) - N_{SE,u}(t)] &= \beta(t) S_u(t) \left[ \left( \frac{I_u + \iota}{P_u} \right)^\alpha \right. \\ &\quad \left. + \sum_{\tilde{u} \neq u} \frac{v_{u\tilde{u}}}{P_u} \left\{ \left( \frac{I_{\tilde{u}}}{P_{\tilde{u}}} \right)^\alpha - \left( \frac{I_u}{P_u} \right)^\alpha \right\} \right] dt + o(dt), \end{aligned} \quad (6)$$

where  $\beta(t)$  models seasonality driven by high contact rates between children at school, described by

$$\beta(t) = \begin{cases} (1 + a(1-p)p^{-1}) \bar{\beta} & \text{during school term,} \\ (1-a) \bar{\beta} & \text{during vacation} \end{cases}$$

with  $p = 0.759$  being the proportion of the year taken up by the school terms,  $\bar{\beta}$  is the mean transmission rate, and  $a$  measures the reduction of transmission during school holidays. In [6],  $\alpha$  is a mixing exponent modeling inhomogeneous contact rates within a city, and  $\iota$  models immigration of infected individuals which is appropriate when analyzing a subset of cities that cannot be treated as a closed system. The number of travelers from city  $u$  to  $\tilde{u}$  is denoted by  $v_{u\tilde{u}}$ . Here,  $v_{u\tilde{u}}$  is constructed using the gravity model of Xia et al. (2004),

$$v_{u\tilde{u}} = G \cdot \frac{\bar{d}}{\bar{P}^2} \cdot \frac{P_u \cdot P_{\tilde{u}}}{d(u, \tilde{u})},$$

where  $d(u, \tilde{u})$  denotes the distance between city  $u$  and city  $\tilde{u}$ ,  $P_u$  is the average population for city  $u$  across time,  $\bar{P}$  is the average population across cities, and  $\bar{d}$  is the average distance between a randomly chosen pair of cities. Here, we model  $v_{u\tilde{u}}$  as fixed through time and symmetric between any two arbitrary cities, though a natural extension would allow for temporal variation and asymmetric movement between two cities. The transition processes  $N_{EI,u}(t)$ ,  $N_{ED,u}(t)$  and  $N_{\bullet D,u}(t)$  are modeled as conditional Poisson processes with per-capita rates



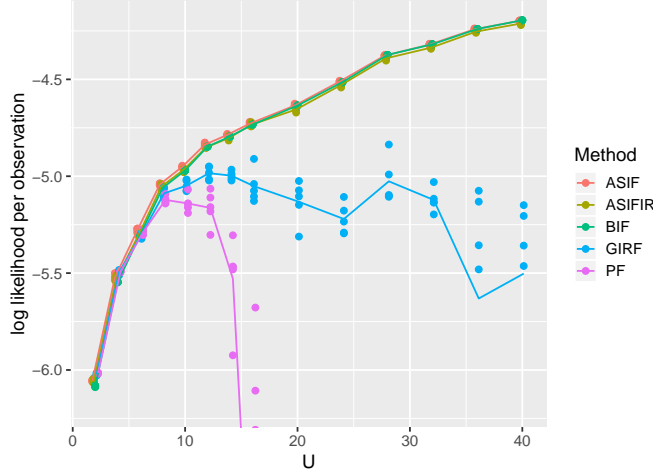


Figure 2: log likelihood estimates for simulated data from the measles model of various dimensions. BIF, ASIF and ASIF-IR are compared with a guided intermediate resampling filter (GIRF) and a basic particle filter (PF).

$\mu_{EI}$ ,  $\mu_{IR}$  and  $\mu_{\bullet D}$  respectively, and we fix  $\mu_{\bullet D} = 50 \text{ year}^{-1}$ . The birth process  $N_{BS,u}(t)$  is an inhomogeneous Poisson processes with rate  $\mu_{BS,u}(t)$ , given by interpolated census data.

To complete the model specification, we must describe the measurement process. Let  $Z_{u,n} = N_{IR,u}(t_n) - N_{IR,u}(t_{n-1})$  be the number of removed infected individuals in the  $n$ th reporting interval. Suppose that cases are quarantined once they are identified, so that reported cases comprise a fraction  $\rho$  of these removal events. The case report  $y_{u,n}^*$  is modeled as a realization of a discretized conditionally Gaussian random variable  $Y_{u,n}$ , defined for  $y > 0$  via

$$\begin{aligned} \mathbb{P}[Y_{u,n}=y \mid Z_{u,n}=z] &= \Phi(y + 0.5; \rho z, \rho(1 - \rho)z + \psi^2 \rho^2 z^2) \\ &\quad - \Phi(y - 0.5; \rho z, \rho(1 - \rho)z + \psi^2 \rho^2 z^2) \end{aligned} \quad (7)$$

where  $\Phi(\cdot; \mu, \sigma^2)$  is the  $\mathcal{N}(\mu, \sigma^2)$  cumulative distribution function, and  $\psi$  models overdispersion relative to the binomial distribution. For  $y = 0$ , we replace  $y - 0.5$  by  $-\infty$  in [7].

This model includes many features that have been proposed to be relevant for understanding measles transmission dynamics He et al. (2010). Our plug-and-play methodology permits consideration of all these features, and readily extends to the investigation of further variations. Likelihood-based inference via plug-and-play methodology therefore provides a framework for evaluating which features of a dynamical model are critical for explaining the data King et al. (2008). By contrast, Xia et al. (2004) developed a linearization for a specific spatiotemporal measles model which is numerically convenient but not readily adaptable to assess alternative model choices.

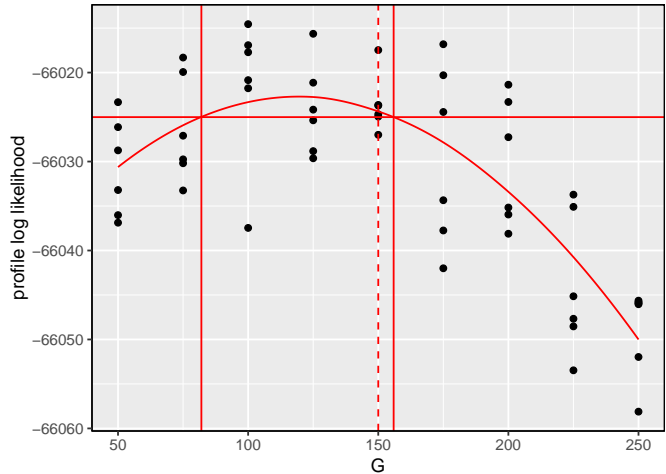


Figure 3: Likelihood slice varying the coupling parameter, computed via ASIF with  $U = 40$  cities. The solid lines construct a 95% Monte Carlo adjusted confidence interval Ionides et al. (2017). For this model realization, this interval includes the true parameter value identified by a dashed line.

We first assess the scaling properties of the filters on the measles model by evaluating the likelihood over varying numbers of units,  $U$ , for fixed parameters. The results are given in Fig. 2, with additional information about timing, algorithmic choices, parameter values and a plot of the data provided in Sec. S6. In Fig. 2, the log likelihood per unit per time increases with  $U$  because city size decreases with  $U$ . Smaller cities have fewer measles cases, resulting in a narrower and taller probability density function. Fig. 2 shows all three island filters performing well, compared to a rapid decline in performance of the particle filter (PF) starting at  $U = 10$ , and a slower decline for GIRF. The bias in the island filters is small in this example, as evidenced by their close match to PF for small numbers of units. This is likely because the coupling in this model is weak: a high proportion of measles transmission occurs within cities rather than between cities. The neighborhood used here for city  $u$  at time  $n$  was two previous lags,  $\{(u, n - 1), (u, n - 2)\}$ . This choice of neighborhood is explored in Sec. S7. This local neighborhood still involves other cities in forecast for city  $u$ , since the forecast on each island involves a full coupled model.

Fig. 3 evaluates the filter methods on the task of computing a slice of the likelihood function over the coupling parameter  $G$  for simulated data. This slice varies  $G$  while fixing the other parameters at the values used for the simulation. Scientifically, this gives us an upper bound on the identifiability of  $G$  from such data, since the likelihood slice provides statistically efficient inference when all other parameters are known. In this case, the Monte Carlo error is comparable to the change in the log likelihood over a wide range of values of  $G$ . Therefore, Monte Carlo error has substantial impact on inference even given considerable

computational resources: Fig. 3 took 7 days to compute on 40 cores. Most transmission of measles is local, so evidently there is limited evidence available about strength of transmission between cities even from 40 jointly observed epidemic time series. By contrast, parameters of within-city transmission that are shared between cities should be well identified by carrying out inference on a collection of cities. As an example of this, Sec. S8 presents a likelihood slice for the recovery rate,  $\mu_{IR}$ .

## Discussion

The pseudocode presented for the island filters describes how the outputs are calculated given the inputs, but does not prescribe details of how these quantities are calculated. There is scope for implementations to trade off memory, computation and communication by making differing decisions on how the various loops defined in the pseudocode are coded, such as decisions on memory over-writing and parallelization. This article focuses on the logical structure of the algorithms, leaving room for future research on implementation-specific considerations, though some supplementary discussion of memory-efficient implementation is given in Sec. S10.

This paper has focused on likelihood evaluation, a critical quantity for testing scientific hypotheses about model structure and the values of unknown parameters. However, our island filters also provide localized solutions to the filtering problem, using the local weights constructed for the adapted simulations constructed on each island. A solution to the filtering problem, in turn, provides a foundation for forecasting.

Plug-and-play inference algorithms based on sequential Monte Carlo likelihood evaluation has proved successful for investigating highly nonlinear partially observed dynamic systems of low dimension arising in analysis of epidemiological and ecological time series data Bretó (2018); Pons-Salort and Grassly (2018); de Cellès et al. (2018); Marino et al. (2018). A benefit of the plug-and-play property is that it facilitates development of broadly applicable software, which in turn promotes creative scientific model development Bretó et al. (2009); He et al. (2010).

Geophysical data assimilation has similarities to inference on spatiotemporal biological systems. Relative to biological systems, geophysical applications are characterized by a greater number of spatial locations, better mathematical understanding of the underlying processes, and lower stochasticity. The locally weighted particle filter of Poterjoy (2016) shares some features with our approach, but it builds on a moment approximation designed for geophysical models.

The algorithms BIF, ASIF, ASIF-IR and GIRF used for this article all enjoy the plug-and-play property. The numerical results for this paper use the `asif`, `asifir` and `girf` functions via the open-source R package `spatPomp` Asfaw et al. (2019) that provides a spatiotemporal extension of the R package `pomp` King et al. (2016). BIF was implemented using `asif` with  $J = 1$  particles per

island. The `pfilter` and `enkf` functions were used from `pomp`. The source code for this paper will be contributed to an open-source scientific archive upon acceptance for publication.

**Acknowledgements:** This work was supported by National Science Foundation grant DMS-1761603 and National Institutes of Health grants 1-U54-GM111274 and 1-U01-GM110712.

## References

- Ades, M. and Van Leeuwen, P. J. (2015). The equivalent-weights particle filter in a high-dimensional system, *Quarterly Journal of the Royal Meteorological Society* **141**(687): 484–503.
- Andrieu, C., Doucet, A. and Holenstein, R. (2010). Particle Markov chain Monte Carlo methods, *Journal of the Royal Statistical Society, Series B (Statistical Methodology)* **72**: 269–342.
- Asfaw, K., Ionides, E. L. and King, A. A. (2019). `spatPomp`: R package for statistical inference for spatiotemporal partially observed Markov processes, <https://github.com/kidusasfaw/spatPomp> .
- Bengtsson, T., Bickel, P. and Li, B. (2008). Curse-of-dimensionality revisited: Collapse of the particle filter in very large scale systems, in T. Speed and D. Nolan (eds), *Probability and Statistics: Essays in Honor of David A. Freedman*, Institute of Mathematical Statistics, Beachwood, OH, pp. 316–334.
- Bjørnstad, O. N. and Grenfell, B. T. (2001). Noisy clockwork: Time series analysis of population fluctuations in animals, *Science* **293**: 638–643.
- Bretó, C. (2018). Modeling and inference for infectious disease dynamics: A likelihood-based approach, *Statistical Science* **33**(1): 57–69.
- Bretó, C., He, D., Ionides, E. L. and King, A. A. (2009). Time series analysis via mechanistic models, *Annals of Applied Statistics* **3**: 319–348.
- Bretó, C. and Ionides, E. L. (2011). Compound Markov counting processes and their applications to modeling infinitesimally over-dispersed systems, *Stochastic Processes and their Applications* **121**: 2571–2591.
- Crisan, D. and Rozovskii, B. (2011). *The Oxford handbook of nonlinear filtering*, Oxford University Press.
- de Cellès, M. D., Magpantay, F. M., King, A. A. and Rohani, P. (2018). The impact of past vaccination coverage and immunity on pertussis resurgence, *Science Translational Medicine* **10**(434): eaa1748.
- Del Moral, P., Moulines, E., Olsson, J. and Vergé, C. (2017). Convergence properties of weighted particle islands with application to the double bootstrap algorithm, *Stochastic Systems* **6**(2): 367–419.

- Del Moral, P. and Murray, L. M. (2015). Sequential Monte Carlo with highly informative observations, *Journal on Uncertainty Quantification* **3**: 969–997.
- Doucet, A., de Freitas, N. and Gordon, N. J. (2001). *Sequential Monte Carlo Methods in Practice*, Springer, New York.
- Doucet, A. and Johansen, A. (2011). A tutorial on particle filtering and smoothing: Fifteen years later, in D. Crisan and B. Rozovsky (eds), *Oxford Handbook of Nonlinear Filtering*, Oxford University Press.
- Ebert, E. E. (2001). Ability of a poor man’s ensemble to predict the probability and distribution of precipitation, *Monthly Weather Review* **129**(10): 2461–2480.
- He, D., Ionides, E. L. and King, A. A. (2010). Plug-and-play inference for disease dynamics: Measles in large and small towns as a case study, *Journal of the Royal Society Interface* **7**: 271–283.
- Ionides, E. L., Breto, C., Park, J., Smith, R. A. and King, A. A. (2017). Monte Carlo profile confidence intervals for dynamic systems, *Journal of the Royal Society Interface* **14**: 1–10.
- Ionides, E. L., Nguyen, D., Atchadé, Y., Stoev, S. and King, A. A. (2015). Inference for dynamic and latent variable models via iterated, perturbed Bayes maps, *Proceedings of the National Academy of Sciences of the USA* **112**(3): 719–724.
- King, A. A., Ionides, E. L., Pascual, M. and Bouma, M. J. (2008). Inapparent infections and cholera dynamics, *Nature* **454**: 877–880.
- King, A. A., Nguyen, D. and Ionides, E. L. (2016). Statistical inference for partially observed Markov processes via the R package pomp, *Journal of Statistical Software* **69**: 1–43.
- Leutbecher, M. and Palmer, T. N. (2008). Ensemble forecasting, *Journal of Computational Physics* **227**(7): 3515–3539.
- Marino, J. A., Peacor, S. D., Bunnell, D. B., Vanderploeg, H. A., Pothoven, S. A., Elgin, A. K., Bence, J. R., Jiao, J. and Ionides, E. L. (2018). Evaluating consumptive and nonconsumptive predator effects on prey density using field times series data, *Ecology* .
- Palmer, T. N. (2002). The economic value of ensemble forecasts as a tool for risk assessment: From days to decades, *Quarterly Journal of the Royal Meteorological Society* **128**(581): 747–774.
- Park, J. and Ionides, E. L. (2019). Inference on high-dimensional implicit dynamic models using a guided intermediate resampling filter, *Arxiv:1708.08543v3* .

- Pitt, M. K. and Shepard, N. (1999). Filtering via simulation: Auxillary particle filters, *Journal of the American Statistical Association* **94**: 590–599.
- Pons-Salort, M. and Grassly, N. C. (2018). Serotype-specific immunity explains the incidence of diseases caused by human enteroviruses, *Science* **361**(6404): 800–803.
- Poterjoy, J. (2016). A localized particle filter for high-dimensional nonlinear systems, *Monthly Weather Review* **144**(1): 59–76.
- Rebeschini, P. and van Handel, R. (2015). Can local particle filters beat the curse of dimensionality?, *The Annals of Applied Probability* **25**(5): 2809–2866.
- Snyder, C., Bengtsson, T. and Morzfeld, M. (2015). Performance bounds for particle filters using the optimal proposal, *Monthly Weather Review* **143**(11): 4750–4761.
- Vergé, C., Dubarry, C., Del Moral, P. and Moulines, E. (2013). On parallel implementation of sequential Monte Carlo methods: The island particle model, *Statistics and Computing* **25**(2): 243–260.
- Xia, Y., Bjørnstad, O. N. and Grenfell, B. T. (2004). Measles metapopulation dynamics: A gravity model for epidemiological coupling and dynamics, *American Naturalist* **164**(2): 267–281.

# Island filters for partially observed spatiotemporal systems

E. L. Ionides, K. Asfaw, J. Park and A. A. King

June 11, 2022

## Supplementary Content

<b>S1</b>	<b>A generalization to models without latent unit structure</b>	<b>2</b>
<b>S2</b>	<b>Adapted simulation for an Euler approximation</b>	<b>3</b>
<b>S3</b>	<b>BIF convergence: Proof of Theorem 1</b>	<b>6</b>
<b>S4</b>	<b>ASIF and ASIF-IR convergence: Proof of Theorem 2</b>	<b>10</b>
<b>S5</b>	<b>The correlated Brownian motion example</b>	<b>18</b>
<b>S6</b>	<b>The measles example</b>	<b>20</b>
<b>S7</b>	<b>Varying the neighborhood for measles</b>	<b>23</b>
<b>S8</b>	<b>A likelihood slice across recovery rate for the measles model</b>	<b>24</b>
<b>S9</b>	<b>A Lorenz '96 example</b>	<b>25</b>
<b>S10</b>	<b>A memory-efficient representation of ASIF</b>	<b>28</b>

## S1 A generalization to models without latent unit structure

Variations of the algorithms in the main text apply when there is no latent unit structure. In this case, the observation vector  $\mathbf{Y}_n = (Y_{1,n}, \dots, Y_{U,n})$  consists of a collection of measurements on a general latent vector  $X_n$ . We may have the structure that  $Y_{1,n}, \dots, Y_{U,n}$  are conditionally independent given  $X_n$ , but even this is not essential to the approach. This is most readily seen in the context of the basic island filter, giving rise to the generalized basic island filter (G-BIF) algorithm defined as follows.

---

### Algorithm G-BIF (Generalized basic island filter).

---

**input:**

Simulator for  $f_{X_n|X_{n-1}}(x_n|x_{n-1})$

Evaluator for  $f_{Y_{u,n}|X_n}(y_{u,n}^*|x_n)$

Number of islands,  $\mathcal{I}$

Neighborhood structure,  $B_{u,n}$ , for  $u \in 1:U$  and  $n \in 1:N$

Data,  $y_{u,n}^*$  for  $u \in 1:U$  and  $n \in 1:N$

**output:**

Log likelihood estimate,  $\ell^{\text{MC}} = \sum_{n=1}^N \sum_{u=1}^U \ell_{u,n}^{\text{MC}}$

---

For  $i$  in  $1:\mathcal{I}$

simulate  $X_{n,i}^{\text{sim}}$  from the dynamic model, for  $n \in 1:N$

End For

Prediction weights,  $w_{u,n,i}^P = f_{Y_{B_{u,n}}|X_{1:n}}(y_{B_{u,n}}^*|X_{1:n,i}^{\text{sim}})$

Measurement weights,  $w_{u,n,i}^M = f_{Y_{u,n}|X_n, Y_{B_{u,n}}}(y_{u,n}^*|X_{n,i}^{\text{sim}}, y_{B_{u,n}}^*)$

Conditional log likelihood estimate,  $\ell_{u,n}^{\text{MC}} = \log \left( \sum_{i=1}^{\mathcal{I}} w_{u,n,i}^M w_{u,n,i}^P \right) - \log \left( \sum_{\tilde{i}=1}^{\mathcal{I}} w_{u,n,\tilde{i}}^P \right)$

---

The algorithm G-BIF operates on an arbitrary POMP model. G-BIF therefore provides a potential approach to extending methodologies from SpatPOMP models to models that have some similarity to a SpatPOMP without formally meeting the definition. For example, there may be collections of interacting processes at different spatial scales in a spatiotemporal system. Alternatively, the potential outcomes of the latent process may vary between spatial units, such as when modeling interactions between terrestrial and aquatic ecosystems. We do not further explore G-BIF here.



## S2 Adapted simulation for an Euler approximation

We investigate the adapted simulation process by considering a continuous-time limit where it becomes a diffusion process. We find that adapted simulation can effectively track the latent process when the measurement error is on an appropriate scale. However, when the measurement error is large compared to the latent process noise, adapted simulation can fail in situations where filtering succeeds. We work with a one-dimensional POMP model having a latent process constructed as an Euler approximation,

$$X_{n+1} = X_n + \mu(X_n)\delta + \sigma\sqrt{\delta}\epsilon_{n+1}, \quad (\text{S1})$$

which provides a numerical solution to a one-dimensional stochastic differential equation,

$$dX(t) = \mu(X(t)) dt + \sigma dU(t),$$

where  $\{U(t)\}$  is a standard Brownian motion. We will consider several different measurement processes.

### S2.1 Measurement error on the same scale as the process noise

Here, we consider the measurement model

$$Y_{n+1} = \mu(X_n)\delta + \sigma\sqrt{\delta}\epsilon_{n+1} + \tau\sqrt{\delta}\eta_{n+1}. \quad (\text{S2})$$

This is an approximation to the increment  $Y(t+\delta) - Y(t)$  of a continuous time measurement model

$$dY(t) = dX(t) + \tau dV(t), \quad (\text{S3})$$

where  $\{V(t)\}$  is a standard Brownian motion independent of  $\{U(t)\}$ . The measurement model (S3) makes inference on  $X(t)$  given  $Y(t)$  a continuous time version of the filtering problem. A feature of this model is that  $Y(t)$  does not directly track the level of the state, since the solution with initial conditions  $Y(t_0) = X(t_0)$  and  $V(t_0) = 0$  is

$$Y(t) = X(t) + \tau V(t).$$

The measurement error,  $\tau V(t)$ , has variance  $\tau^2 t$  that increases with  $t$ . However, under appropriate conditions, information on changes in  $\{X(t)\}$  obtained via  $\{Y(t)\}$  are enough to track  $X(t)$  indirectly via the filtering equations. For the POMP given by (S1) and (S2), we can calculate exactly the adapted simulation distribution  $f_{X_{n+1}|Y_{n+1}, X_n}$ . It is convenient to work conditionally on  $X_n$ , allowing us to treat  $X_n$  and  $\mu(X_n)$  as constants, with  $X_{n+1}$  and  $Y_{n+1}$  therefore being jointly normally distributed. A Gaussian distribution calculation then gives the conditional moments. First, we find

$$\begin{aligned} \mathbb{E}[X_{n+1}|Y_{n+1}, X_n] &= X_n + \mu(X_n)\delta + \mathbb{E}[\sigma\sqrt{\delta}\epsilon_{n+1} \mid \sigma\sqrt{\delta}\epsilon_{n+1} + \tau\sqrt{\delta}\eta_{n+1}] \\ &= X_n + \mu(X_n)\delta + \frac{\sigma^2}{\sigma^2 + \tau^2}(\sigma\sqrt{\delta}\epsilon_{n+1} + \tau\sqrt{\delta}\eta_{n+1}) \\ &= X_n + \mu(X_n)\delta + \frac{\sigma^2}{\sigma^2 + \tau^2}(Y_{n+1} - \mu(X_n)\delta). \end{aligned}$$

Then,

$$\begin{aligned}
\text{Var}[X_{n+1} | Y_{n+1}, X_n] &= \text{Var}[\sigma\sqrt{\delta}\epsilon_{n+1} | \sigma\sqrt{\delta}\epsilon_{n+1} + \tau\sqrt{\delta}\eta_{n+1}] \\
&= \sigma^2\delta - \frac{\sigma^4\delta^2}{\sigma^2\delta + \tau^2\delta} \\
&= \delta \frac{\sigma^2\tau^2}{\sigma^2 + \tau^2}.
\end{aligned}$$

Call the adapted simulation process  $\{A_n\}$ , defined conditionally on  $\{Y_n\}$ . We see from the above calculation that

$$\begin{aligned}
A_{n+1} &= A_n + \mu(A_n)\delta + \frac{\sigma^2}{\sigma^2 + \tau^2} \left( \mu(X_n)\delta + \sigma\sqrt{\delta}\epsilon_{n+1} + \tau\sqrt{\delta}\eta_{n+1} - \mu(A_n)\delta \right) \\
&\quad + \frac{\sigma\tau}{\sqrt{\sigma^2 + \tau^2}} \sqrt{\delta}\zeta_{n+1}
\end{aligned}$$

where  $\{\zeta_n\}$  is an iid standard normal sequence independent of  $\{\epsilon_n, \eta_n\}$ . To study how well the adapted simulation tracks  $\{X_n\}$ , we subtract  $X_{n+1}$  from both sides to get

$$\begin{aligned}
[A_{n+1} - X_{n+1}] &= [A_n - X_n] + [\mu(A_n) - \mu(X_n)]\delta - \sigma\sqrt{\delta}\epsilon_{n+1} \\
&\quad + \frac{\sigma^2}{\sigma^2 + \tau^2} \left( [\mu(X_n) - \mu(A_n)]\delta + \sigma\sqrt{\delta}\epsilon_{n+1} + \tau\sqrt{\delta}\eta_{n+1} \right) + \frac{\sigma\tau}{\sqrt{\sigma^2 + \tau^2}} \sqrt{\delta}\zeta_{n+1} \\
&= [A_n - X_n] + \frac{2\sigma^2 + \tau^2}{\sigma^2 + \tau^2} [\mu(X_n) - \mu(A_n)]\delta \\
&\quad + \frac{\sigma^2\tau\sqrt{\delta}\eta_{n+1} - \sigma\tau^2\sqrt{\delta}\epsilon_{n+1}}{\sigma^2 + \tau^2} + \frac{\sigma\tau}{\sqrt{\sigma^2 + \tau^2}} \sqrt{\delta}\zeta_{n+1}.
\end{aligned}$$

$\{A_n\}$  tracks  $\{X_n\}$  when the process  $\{A_n - X_n\}$  is stable. This happens when  $\mu(x) - \mu(y)$  is negative when  $x$  is sufficiently larger than  $y$ . For example, a stable autoregressive process with  $\mu(x) = -ax$  gives a stable adapted filter process.

## S2.2 Independent measurement error on a scale that gives a finite limiting amount of information about $X(t)$ from measurements on a unit time interval

We now consider the measurement model

$$\begin{aligned}
Y_{n+1} &= X_{n+1} + \frac{\tau}{\sqrt{\delta}} \eta_{n+1} \\
&= X_n + \mu(X_n)\delta + \sigma\sqrt{\delta}\epsilon_{n+1} + \frac{\tau}{\sqrt{\delta}} \eta_{n+1},
\end{aligned} \tag{S4}$$

where  $\{\epsilon_n, \eta_n\}$  is a collection of independent standard normal random variables. The conditional mean is now

$$\begin{aligned}
\mathbb{E}[X_{n+1} | Y_{n+1}, X_n] &= X_n + \mu(X_n)\delta + \mathbb{E}\left[\sigma\sqrt{\delta}\epsilon_{n+1} \mid \sigma\sqrt{\delta}\epsilon_{n+1} + \frac{\tau}{\sqrt{\delta}}\eta_{n+1}\right] \\
&= X_n + \mu(X_n)\delta + \frac{\sigma^2\delta}{\sigma^2\delta + \tau^2/\delta} (\sigma\sqrt{\delta}\epsilon_{n+1} + \tau\sqrt{\delta}\eta_{n+1})
\end{aligned} \tag{S5}$$

Using (S4) and (S5) gives

$$\mathbb{E}[X_{n+1}|Y_{n+1}, X_n] = X_n + \mu(X_n)\delta + \frac{\sigma^2\delta^2}{\sigma^2\delta^2 + \tau^2} (Y_{n+1} - X_n - \mu(X_n)\delta).$$

In the limit as  $\delta \rightarrow 0$ , the contribution from the measurement is order  $\delta^2$  and is therefore negligible. Although the observation process is meaningfully informative about the latent process, the adapted simulation fails to track the latent process in this limit. Intuitively, this is because the adapted simulation is trying to track differences in the latent process, but for this model the signal to noise ratio for the difference in each interval of length  $\delta$  tends to zero.

### S2.3 Independent measurements of the latent process with measurement error on a scale that gives a useful adapted process as $\delta \rightarrow 0$

We now consider the measurement model

$$\begin{aligned} Y_{n+1} &= X_{n+1} + \tau\eta_{n+1} \\ &= X_n + \mu(X_n)\delta + \sigma\sqrt{\delta}\epsilon_{n+1} + \tau\eta_{n+1}. \end{aligned} \tag{S6}$$

The conditional mean is now

$$\begin{aligned} \mathbb{E}[X_{n+1}|Y_{n+1}, X_n] &= X_n + \mu(X_n)\delta + \mathbb{E}[\sigma\sqrt{\delta}\epsilon_{n+1} | \sigma\sqrt{\delta}\epsilon_{n+1} + \tau\eta_{n+1}] \\ &= X_n + \mu(X_n)\delta + \frac{\sigma^2\delta}{\sigma^2\delta + \tau^2} (\sigma\sqrt{\delta}\epsilon_{n+1} + \tau\eta_{n+1}) \end{aligned} \tag{S7}$$

Using (S6) and (S7) gives

$$\begin{aligned} \mathbb{E}[X_{n+1}|Y_{n+1}, X_n] &= X_n + \mu(X_n)\delta + \frac{\sigma^2\delta}{\sigma^2\delta + \tau^2} (Y_{n+1} - X_n - \mu(X_n)\delta) \\ &= X_n + \mu(X_n)\delta + \frac{\sigma^2}{\tau^2}\delta (Y_{n+1} - X_n - \mu(X_n)\delta) + o(\delta) \end{aligned}$$

In the limit as  $\delta \rightarrow 0$ , the adapted simulation has a diffusive drift toward the value of the latent process.

For disease models, incidence data can arguably be considered as noisy measurements of the change of a state variable (number of susceptibles) that is not directly measured. This could correspond to a situation where the measurement error is on the same scale as the process noise (Subsection S2.1). Alternatively, we could think of weekly aggregated incidence as a noisy measurement of the infected class, in which case the measurement error could match the scaling in Subsection S2.3.

The model in Subsection S2.2 is a cautionary tale, warning us against carrying out adapted simulation on short time intervals. An interpretation is that one should not carry out adapted simulation unless a reasonable amount of information has accrued. When each observation has low information, a particle filter may enable solution to the filtering problem without particle depletion. It is when the data are highly informative that the curse of dimensionality makes basic particle filters ineffective, opening up demand for alternative methods.

### S3 BIF convergence: Proof of Theorem 1

We consider a collection of models  $f_{\mathbf{x}_{0:N}, \mathbf{y}_{1:N}}$  and data  $\mathbf{y}_{1:N}^*$  defined for each  $(U, N)$ . These models and datasets are not required to have any nesting relationship, so we do not insist that  $X_{1,1}$  or  $y_{1,1}^*$  should be the same for  $(U, N) = (10, 10)$  as for  $(U, N) = (100, 100)$ . Formally, we define probability and expectation on a product space of the stochastic model and Monte Carlo outcomes. Monte Carlo quantities such as the output of the TIF, ASIF and ASIF-IR algorithms depend on the data but not on any random variables constructed under the model. As a consequence, we can use  $\mathbb{E}$  to correspond both to expectations over Monte Carlo stochasticity (for Monte Carlo quantities) and model stochasticity (for random variables constructed under the model). We suppress discussion of measurability by assuming that all functions considered have appropriate measurability properties. We restate the assumptions and statement for Theorem 1.

**Assumption A1.** *There is an  $\epsilon_{A1} > 0$  and a collection of neighborhoods  $\{B_{u,n} \subset A_{u,n}, u \in 1:U, n \in 1:N\}$  such that, for all  $u, n, U, N$ , any bounded real-valued function  $|h(x)| \leq 1$ , and any value of  $x_{B_{u,n}^c}$ ,*

$$\left| \int h(x_{u,n}) f_{X_{u,n}|Y_{B_{u,n}}, X_{B_{u,n}^c}}(x_{u,n} | y_{B_{u,n}}^*, x_{B_{u,n}^c}) dx_{u,n} - \int h(x_{u,n}) f_{X_{u,n}|Y_{B_{u,n}}}(x_{u,n} | y_{B_{u,n}}^*) dx_{u,n} \right| < \epsilon_{A1}. \quad (\text{S8})$$

We use the total variation bound in Assumption A1 via the following Proposition S1, which replaces conditioning on  $X_{B_{u,n}^c}$  with conditioning on  $Y_{B_{u,n}^c}$ . The bound in (S9) could be used in place of Assumption A1.

**Proposition S1.** *Under the conditions of Assumption A1, (S8) implies*

$$\left| \int h(x_{u,n}) f_{X_{u,n}|Y_{A_{u,n}}}(x_{u,n} | y_{A_{u,n}}^*) dx_{u,n} - \int h(x_{u,n}) f_{X_{u,n}|Y_{B_{u,n}}}(x_{u,n} | y_{B_{u,n}}^*) dx_{u,n} \right| < \epsilon_{A1} \quad (\text{S9})$$

*Proof.* For notational compactness, we suppress the arguments  $x_{u,n}, x_{B_{u,n}^c}, y_{A_{u,n}}^*, y_{B_{u,n}}^*$  matching the subscripts of conditional densities. Using the conditional independence of the measurements given the latent process, we calculate

$$\begin{aligned} & \left| \int h(x_{u,n}) f_{X_{u,n}|Y_{A_{u,n}}} dx_{u,n} - \int h(x_{u,n}) f_{X_{u,n}|Y_{B_{u,n}}} dx_{u,n} \right| \\ &= \left| \int \left\{ \int h(x_{u,n}) f_{X_{u,n}|Y_{B_{u,n}}, X_{B_{u,n}^c}} dx_{u,n} - \int h(x_{u,n}) f_{X_{u,n}|Y_{B_{u,n}}} dx_{u,n} \right\} f_{X_{B_{u,n}^c}|Y_{A_{u,n}}} dx_{B_{u,n}^c} \right| \\ &\leq \int \left| \int h(x_{u,n}) f_{X_{u,n}|Y_{B_{u,n}}, X_{B_{u,n}^c}} dx_{u,n} - \int h(x_{u,n}) f_{X_{u,n}|Y_{B_{u,n}}} dx_{u,n} \right| f_{X_{B_{u,n}^c}|Y_{A_{u,n}}} dx_{B_{u,n}^c} \\ &< \int \epsilon_{A1} f_{X_{B_{u,n}^c}|Y_{A_{u,n}}} dx_{B_{u,n}^c} = \epsilon_{A1}. \end{aligned}$$

□

**Assumption A2.** For the collection of neighborhoods in Assumption A1, with  $B_{u,n}^+ = B_{u,n} \cup (u, n)$ , there is a constant  $b$ , depending on  $\epsilon_{A1}$  but not on  $U$  and  $N$ , such that

$$\sup_{u \in 1:U, n \in 1:N} |B_{u,n}^+| \leq b.$$

**Assumption A3.** There is a constant  $Q$  such that, for all  $u$  and  $n$ ,  $U$  and  $N$ ,

$$Q^{-1} < f_{Y_{u,n}|X_{u,n}}(y_{u,n}^* | x_{u,n}) < Q$$

**Assumption A4.** There exists  $\epsilon_{A4} > 0$  such that the following holds. For each  $u, n$ , a set  $C_{u,n} \subset (1:U) \times (0:N)$  exists such that  $(\tilde{u}, \tilde{n}) \notin C_{u,n}$  implies  $B_{u,n}^+ \cap B_{\tilde{u},\tilde{n}}^+ = \emptyset$  and

$$|f_{X_{B_{\tilde{u},\tilde{n}}^+}|X_{B_{\tilde{u},\tilde{n}}^+}} - f_{X_{B_{u,n}^+}|X_{B_{u,n}^+}}| < \epsilon_{A4} f_{X_{B_{\tilde{u},\tilde{n}}^+}|X_{B_{\tilde{u},\tilde{n}}^+}} \quad (\text{S10})$$

Further, there is a uniform bound  $|C_{u,n}| \leq c$ .

Assumption A4 is needed only to ensure that the variance bound in Theorem 1 is essentially  $O(UN)$  rather than  $O(U^2N^2)$ . Both these rates avoid the exponentially increasing variance characterizing the curse of dimensionality. Lower variance than  $O(UN)$  cannot be anticipated for any sequential Monte Carlo method since the log likelihood estimate can be written as a sum of  $UN$  terms each of which involves its own sequential Monte Carlo calculation.

**Theorem 1.** Let  $\ell^{MC}$  denote the Monte Carlo likelihood approximation constructed by BIF. Consider a limit with a growing number of islands,  $\mathcal{I} \rightarrow \infty$ , and suppose assumptions A1, A2 and A3. There are quantities  $\epsilon(U, N)$  and  $V(U, N)$ , with bounds  $|\epsilon| < \epsilon_{A1} Q^2$  and  $V < Q^{4b} U^2 N^2$ , such that

$$\mathcal{I}^{1/2} [\ell^{MC} - \ell - \epsilon UN] \xrightarrow[\mathcal{I} \rightarrow \infty]{d} \mathcal{N}[0, V], \quad (\text{S11})$$

where  $\xrightarrow[\mathcal{I} \rightarrow \infty]{d}$  denotes convergence in distribution and  $\mathcal{N}[\mu, \Sigma]$  is the normal distribution with mean  $\mu$  and variance  $\Sigma$ . If additionally Assumption A4 holds, we obtain an improved variance bound

$$V < Q^{4b} UN(c + \epsilon_{A4}(UN - c)). \quad (\text{S12})$$

*Proof.* Suppose the quantities  $w_{u,n,i}^M$  and  $w_{u,n,i}^P$  constructed in Algorithm BIF are considered i.i.d. replicates of jointly defined random variables  $w_{u,n}^M$  and  $w_{u,n}^P$ , for each  $(u, n) \in 1:U \times 1:N$ . Also, write

$$\Delta_{u,n}^{MP} = \frac{1}{\sqrt{\mathcal{I}}} \sum_{i=1}^{\mathcal{I}} (w_{u,n,i}^M w_{u,n,i}^P - \mathbb{E}[w_{u,n}^M w_{u,n}^P]), \quad \Delta_{u,n}^P = \frac{1}{\sqrt{\mathcal{I}}} \sum_{i=1}^{\mathcal{I}} (w_{u,n,i}^P - \mathbb{E}[w_{u,n}^P]),$$

Then, using the delta method (e.g., Section 2.5.3 in Liu (2001)) we find

$$\begin{aligned} \ell_{u,n}^{MC} &= \log \left( \frac{\sum_{i=1}^{\mathcal{I}} w_{u,n,i}^M w_{u,n,i}^P}{\sum_{i=1}^{\mathcal{I}} w_{u,n,i}^P} \right) \\ &= \log \left( \mathbb{E}[w_{u,n}^M w_{u,n}^P] + \mathcal{I}^{-1/2} \Delta_{u,n}^{MP} \right) - \log \left( \mathbb{E}[w_{u,n}^P] + \mathcal{I}^{-1/2} \Delta_{u,n}^P \right) \\ &= \log \left( \frac{\mathbb{E}[w_{u,n}^M w_{u,n}^P]}{\mathbb{E}[w_{u,n}^P]} \right) + \mathcal{I}^{-1/2} \left( \frac{\Delta_{u,n}^{MP}}{\mathbb{E}[w_{u,n}^M w_{u,n}^P]} - \frac{\Delta_{u,n}^P}{\mathbb{E}[w_{u,n}^P]} \right) + o_P(\mathcal{I}^{-1/2}) \end{aligned} \quad (\text{S13})$$

The joint distribution of  $\{(\Delta_{u,n}^{MP}, \Delta_{u,n}^P), (u, n) \in 1:U \times 1:N\}$  follows a standard central limit theorem as  $\mathcal{I} \rightarrow \infty$ . Each term has mean zero, with covariances uniformly bounded over  $(u, n, \tilde{u}, \tilde{n})$  due to Assumption A3. Specifically,

$$\text{Var} \begin{pmatrix} \Delta_{u,n}^{MP} \\ \Delta_{u,n}^P \\ \Delta_{\tilde{u},\tilde{n}}^{MP} \\ \Delta_{\tilde{u},\tilde{n}}^P \end{pmatrix} = \begin{pmatrix} \text{Var}(w_{u,n}^M w_{u,n}^P) & \text{Cov}(w_{u,n}^M w_{u,n}^P, w_{u,n}^P) & \text{Cov}(w_{u,n}^M w_{u,n}^P, w_{\tilde{u},\tilde{n}}^M w_{\tilde{u},\tilde{n}}^P) & \text{Cov}(w_{u,n}^M w_{u,n}^P, w_{\tilde{u},\tilde{n}}^P) \\ \text{Cov}(w_{u,n}^M w_{u,n}^P, w_{u,n}^P) & \text{Var}(w_{u,n}^P) & \text{Cov}(w_{u,n}^P, w_{\tilde{u},\tilde{n}}^M w_{\tilde{u},\tilde{n}}^P) & \text{Cov}(w_{u,n}^P, w_{\tilde{u},\tilde{n}}^P) \\ \text{Cov}(w_{u,n}^M w_{u,n}^P, w_{\tilde{u},\tilde{n}}^M w_{\tilde{u},\tilde{n}}^P) & \text{Cov}(w_{u,n}^P, w_{\tilde{u},\tilde{n}}^M w_{\tilde{u},\tilde{n}}^P) & \text{Var}(w_{\tilde{u},\tilde{n}}^M w_{\tilde{u},\tilde{n}}^P) & \text{Cov}(w_{\tilde{u},\tilde{n}}^M w_{\tilde{u},\tilde{n}}^P, w_{\tilde{u},\tilde{n}}^P) \\ \text{Cov}(w_{u,n}^M w_{u,n}^P, w_{\tilde{u},\tilde{n}}^P) & \text{Cov}(w_{u,n}^P, w_{\tilde{u},\tilde{n}}^P) & \text{Cov}(w_{\tilde{u},\tilde{n}}^M w_{\tilde{u},\tilde{n}}^P, w_{\tilde{u},\tilde{n}}^P) & \text{Var}(w_{\tilde{u},\tilde{n}}^P) \end{pmatrix}$$

Note that

$$\begin{aligned} \log \left[ \frac{\mathbb{E}[w_{u,n}^M w_{u,n}^P]}{\mathbb{E}[w_{u,n}^P]} \right] &= \log \left[ \frac{\int f_{Y_{u,n}|X_{u,n}}(y_{u,n}^* | x_{u,n,i}) f_{Y_{B_{u,n}}|X_{B_{u,n}}}(y_{B_{u,n}}^* | x_{B_{u,n}}) f_{X_{B_{u,n}^+}}(x_{B_{u,n}^+}) dx_{B_{u,n}^+}}{\int f_{Y_{B_{u,n}}|X_{B_{u,n}}}(y_{B_{u,n}}^* | x_{B_{u,n}}) f_{X_{B_{u,n}}}(x_{B_{u,n}}) dx_{B_{u,n}}} \right] \\ &= \log [f_{Y_{u,n}|Y_{B_{u,n}}}(y_{u,n}^* | y_{B_{u,n}}^*)], \end{aligned}$$

where  $B_{u,n}^+ = B_{u,n} \cup (u, n)$ . Now, define

$$\Delta_{u,n}^\ell = \left( \frac{\Delta_{u,n}^{MP}}{\mathbb{E}[w_{u,n}^M w_{u,n}^P]} - \frac{\Delta_{u,n}^P}{\mathbb{E}[w_{u,n}^P]} \right)$$

Summing over all  $(u, n) \in 1:U \times 1:N$ , we get

$$\sqrt{\mathcal{I}} \left( \ell^{\text{MC}} - \sum_{(u,n) \in 1:U \times 1:N} \log f_{Y_{u,n}|Y_{B_{u,n}}}(y_{u,n}^* | y_{B_{u,n}}^*) \right) = \sum_{(u,n) \in 1:U \times 1:N} \Delta_{u,n}^\ell + o(1). \quad (\text{S14})$$

Now,

$$\text{Cov}(\Delta_{u,n}^\ell, \Delta_{\tilde{u},\tilde{n}}^\ell) = \text{Cov} \left( \frac{w_{u,n}^M w_{u,n}^P}{\mathbb{E}[w_{u,n}^M w_{u,n}^P]} - \frac{w_{u,n}^P}{\mathbb{E}[w_{u,n}^P]}, \frac{w_{\tilde{u},\tilde{n}}^M w_{\tilde{u},\tilde{n}}^P}{\mathbb{E}[w_{\tilde{u},\tilde{n}}^M w_{\tilde{u},\tilde{n}}^P]} - \frac{w_{\tilde{u},\tilde{n}}^P}{\mathbb{E}[w_{\tilde{u},\tilde{n}}^P]} \right).$$

Since

$$\left| \frac{w_{u,n}^M w_{u,n}^P}{\mathbb{E}[w_{u,n}^M w_{u,n}^P]} - \frac{w_{u,n}^P}{\mathbb{E}[w_{u,n}^P]} \right| < Q^{2b},$$

we have

$$|\text{Cov}(\Delta_{u,n}^\ell, \Delta_{\tilde{u},\tilde{n}}^\ell)| < Q^{4b},$$

implying that

$$\text{Var} \left( \sum_{(u,n) \in 1:U \times 1:N} \Delta_{u,n}^\ell \right) < Q^{4b} U^2 N^2. \quad (\text{S15})$$

If, in addition,  $(u, n)$  and  $(\tilde{u}, \tilde{n}) \in A_{u,n}$  are sufficiently separated in the sense of Assumption A4, then Lemma S1 shows that Assumption A4 implies

$$|\text{Cov}(\Delta_{u,n}^\ell, \Delta_{\tilde{u},\tilde{n}}^\ell)| < \epsilon_{A4} Q^{4b}.$$

The number of insufficiently separated neighbors to  $(u, n)$  is bounded by  $c$ , and so we obtain

$$\text{Var} \left( \sum_{(u,n) \in \mathcal{S}} \Delta_{u,n}^\ell \right) < Q^{4b} UN (c + \epsilon_{A4} (UN - c)). \quad (\text{S16})$$

Now we proceed to bound the bias in the Monte Carlo central limit estimator of  $\ell$ . Putting  $h(x_{u,n}) = f_{Y_{u,n}|X_{u,n}}(y_{u,n}^* | x_{u,n})$  into Assumption A1, using Assumption A3, gives

$$|f_{Y_{u,n}|Y_{B_{u,n}}}(y_{u,n}^* | y_{B_{u,n}}^*) - f_{Y_{u,n}|Y_{A_{u,n}}}(y_{u,n}^* | y_{A_{u,n}}^*)| < \epsilon_{A1} Q.$$

Noting that

$$|a - b| < \delta, \quad a > Q^{-1} \text{ and } b > Q^{-1} \text{ implies } |\log(a) - \log(b)| < \delta Q, \quad (\text{S17})$$

we find

$$|\log f_{Y_{u,n}|Y_{B_{u,n}}}(y_{u,n}^* | y_{B_{u,n}}^*) - \log f_{Y_{u,n}|Y_{A_{u,n}}}(y_{u,n}^* | y_{A_{u,n}}^*)| < \epsilon_{A1} Q^2. \quad (\text{S18})$$

Summing over  $(u, n)$ , we get

$$\left| \ell - \sum_{(u,n) \in \mathcal{S}} \log f_{Y_{u,n}|Y_{B_{u,n}}}(y_{u,n}^* | y_{B_{u,n}}^*) \right| < \epsilon_{A1} Q^2 UN. \quad (\text{S19})$$

Together, the results in [S14], [S15], [S16] and [S19] confirm the assertions of the theorem.  $\square$

**Lemma S1.** *Suppose  $U$  and  $V$  are random variables with joint density satisfying*

$$|f_{V|U}(v | u) - f_V(v)| < \epsilon f_V(v). \quad (\text{S20})$$

*Suppose  $|g(U)| < a$  and  $|h(V)| < b$  for some real-valued function  $g$  and  $h$ . Then,  $\text{Cov}(g(U), h(V)) < ab\epsilon$ .*

*Proof.* The result is obtained by direct calculation, as follows.

$$\begin{aligned} \text{Cov}(g(U), h(V)) &= \mathbb{E} \left[ g(U) \mathbb{E} \left[ h(V) - \mathbb{E}[h(V)] \mid U \right] \right] \\ &= \int \left\{ \int g(u) h(v) (f_{V|U}(v | u) - f_V(v)) dv \right\} f_U(u) du \\ &< \int \left\{ \int ab\epsilon f_V(v) dv \right\} f_U(u) du \\ &= ab\epsilon. \end{aligned}$$

$\square$

## S4 ASIF and ASIF-IR convergence: Proof of Theorem 2

Let  $g_{\mathbf{X}_{0:N}, \mathbf{X}_{1:N}^P}(\mathbf{x}_{0:N}, \mathbf{x}_{1:N}^P)$  be the joint density of the adapted process and the proposal process,

$$g_{\mathbf{X}_{0:N}, \mathbf{X}_{1:N}^P}(\mathbf{x}_{0:N}, \mathbf{x}_{1:N}^P) = f_{\mathbf{X}_0}(\mathbf{x}_0) \prod_{n=1}^N f_{\mathbf{X}_n | \mathbf{X}_{n-1}, \mathbf{Y}_n}(\mathbf{x}_n | \mathbf{x}_{n-1}, \mathbf{y}_n^*) f_{\mathbf{X}_n | \mathbf{X}_{n-1}}(\mathbf{x}_n^P | \mathbf{x}_{n-1}). \quad (\text{S21})$$

For  $B \subset 1:U \times 1:N$ , define  $B^{[m]} = B \cap (1:U \times \{m\})$  and set

$$\gamma_B = \prod_{m=1}^N f_{Y_{B^{[m]} | \mathbf{X}_{m-1}}}(y_{B^{[m]}}^* | \mathbf{X}_{m-1}), \quad (\text{S22})$$

using the convention that an empty density  $f_{Y_\emptyset}$  evaluates to 1. If we denoting  $\mathbb{E}_g$  for expectation for  $(\mathbf{X}_{0:N}, \mathbf{X}_{1:N}^P)$  having density  $g_{\mathbf{X}_{0:N}, \mathbf{X}_{1:N}^P}$ , (S22) can be written as

$$\gamma_B = \mathbb{E}_g \left[ f_{Y_B | X_B}(y_B^* | X_B^P) \mid \mathbf{X}_{0:N} \right],$$

so we have

$$\mathbb{E}_g[\gamma_B] = \mathbb{E}_g \left[ f_{Y_B | X_B}(y_B^* | X_B^P) \right].$$

Two useful identities are

$$f_{X_{u,n} | Y_{A_{u,n}}}(x_{u,n} | y_{A_{u,n}}^*) = \frac{\mathbb{E}_g \left[ f_{Y_{A_{u,n}} | X_{A_{u,n}}}(y_{A_{u,n}}^* | X_{A_{u,n}}^P) f_{X_{u,n} | X_{A_{u,n}}^{[n]}, \mathbf{X}_{n-1}}(x_{u,n} | X_{A_{u,n}}^{[n]}, \mathbf{X}_{n-1}) \right]}{\mathbb{E}_g \left[ f_{Y_{A_{u,n}} | X_{A_{u,n}}}(y_{A_{u,n}}^* | X_{A_{u,n}}^P) \right]},$$

$$f_{Y_{u,n} | Y_{A_{u,n}}}(y_{u,n}^* | y_{A_{u,n}}^*) = \frac{\mathbb{E}_g[\gamma_{A_{u,n}^+}]}{\mathbb{E}_g[\gamma_{A_{u,n}}]}.$$

**Assumption B1.** *There is an  $\epsilon_{B1} > 0$  and a collection of neighborhoods  $\{B_{u,n} \subset A_{u,n}, u \in 1:U, n \in 1:N\}$  such that the following holds for all  $u, n, U, N$ , and any bounded real-valued function  $|h(x)| \leq 1$ : if we write  $A = A_{u,n}$ ,  $B = B_{u,n}$ ,  $f_A(x_A) = f_{Y_A | X_A}(y_A^* | x_A)$ , and  $f_B(x_B) = f_{Y_B | X_B}(y_B^* | x_B)$ ,*

$$\left| \int h(x) \left\{ \frac{\mathbb{E}_g[f_A(X_A^P) f_{X_{u,n} | X_{A_{u,n}}^{[n]}, \mathbf{X}_{n-1}}(x | X_{A_{u,n}}^{[n]}, \mathbf{X}_{n-1})]}{\mathbb{E}_g[f_A(X_A^P)]} - \frac{\mathbb{E}_g[f_B(X_B^P) f_{X_{u,n} | X_{B_{u,n}}^{[n]}, \mathbf{X}_{n-1}}(x | X_{B_{u,n}}^{[n]}, \mathbf{X}_{n-1})]}{\mathbb{E}_g[f_B(X_B^P)]} \right\} dx \right| < \epsilon_{B1}.$$

**Assumption B2.** *The bound  $\sup_{u \in 1:U, n \in 1:N} |B_{u,n}^+| \leq b$  in Assumption A2 applies for the neighborhoods defined in Assumption B1. This also implies there is a finite maximum temporal depth for the collection of neighborhoods, defined as*

$$d_{\max} = \sup_{(u,n)} \sup_{(\tilde{u}, \tilde{n}) \in B_{u,n}} |n - \tilde{n}|.$$

**Assumption B3.** *Identically to Assumption A3,  $Q^{-1} < f_{Y_{u,n} | X_{u,n}}(y_{u,n}^* | x_{u,n}) < Q$ .*



**Proposition S2.** Setting  $h(x) = f_{Y_{u,n}|X_{u,n}}(y_{u,n}^*|x)$ , assumptions B1 and B3 imply

$$\left| \frac{\mathbb{E}_g[\gamma_{A_{u,n}^+}]}{\mathbb{E}_g[\gamma_{A_{u,n}}]} - \frac{\mathbb{E}_g[\gamma_{B_{u,n}^+}]}{\mathbb{E}_g[\gamma_{B_{u,n}}]} \right| < Q\epsilon. \quad (\text{S23})$$

*Proof.* Using the nonnegativity of all terms to justify interchange of integral and expectation,

$$\begin{aligned} & \int h(x) \mathbb{E}_g \left[ f_{Y_{B_{u,n}}|X_{B_{u,n}}} (y_{B_{u,n}}^* | X_{B_{u,n}}^P) f_{X_{u,n}|X_{B_{u,n}^{[n]}}, \mathbf{X}_{n-1}} (x | X_{B_{u,n}^{[n]}}, \mathbf{X}_{n-1}) \right] dx \\ &= \mathbb{E}_g \left[ \int f_{Y_{u,n}|X_{u,n}} (y_{u,n}^* | x) f_{X_{u,n}|X_{B_{u,n}^{[n]}}, \mathbf{X}_{n-1}} (x | X_{B_{u,n}^{[n]}}, \mathbf{X}_{n-1}) dx \cdot f_{Y_{B_{u,n}}|X_{B_{u,n}}} (y_{B_{u,n}}^* | X_{B_{u,n}}^P) \right] \end{aligned} \quad (\text{S24})$$

But by the construction of  $g$ ,

$$\begin{aligned} f_{X_{u,n}|X_{B_{u,n}^{[n]}}, \mathbf{X}_{n-1}} (x | X_{B_{u,n}^{[n]}}, \mathbf{X}_{n-1}) &= g_{X_{u,n}^P | X_{B_{u,n}^{[n]}}, \mathbf{X}_{n-1}} (x | X_{B_{u,n}^{[n]}}, \mathbf{X}_{n-1}) \\ &= g_{X_{u,n}^P | X_{B_{u,n}}^P, \mathbf{X}_{n-1}} (x | X_{B_{u,n}}^P, \mathbf{X}_{n-1}). \end{aligned}$$

Thus (S24) becomes

$$\begin{aligned} & \mathbb{E}_g \left[ \int f_{Y_{u,n}|X_{u,n}} (y_{u,n}^* | x) g_{X_{u,n}^P | X_{B_{u,n}}^P, \mathbf{X}_{n-1}} (x | X_{B_{u,n}}^P, \mathbf{X}_{n-1}) dx \cdot f_{Y_{B_{u,n}}|X_{B_{u,n}}} (y_{B_{u,n}}^* | X_{B_{u,n}}^P) \right] \\ &= \mathbb{E}_g \left[ \mathbb{E}_g \left[ f_{Y_{u,n}|X_{u,n}} (y_{u,n}^* | X_{u,n}^P) | X_{B_{u,n}}^P, \mathbf{X}_{n-1} \right] \cdot f_{Y_{B_{u,n}}|X_{B_{u,n}}} (y_{B_{u,n}}^* | X_{B_{u,n}}^P) \right] \\ &= \mathbb{E}_g \left[ f_{Y_{B_{u,n}^+}|X_{B_{u,n}^+}} (y_{B_{u,n}^+}^* | X_{B_{u,n}^+}^P) \right] \\ &= \mathbb{E}_g \gamma_{B_{u,n}^+}. \end{aligned}$$

Applying the same argument for the special case of  $B_{u,n} = A_{u,n}$ , we substitute into Assumption B1 to complete the proof with the fact that  $h < Q$ .  $\square$

**Assumption B4.** Define  $g_{X_A|X_B}$  via (S21). Suppose there is an  $\epsilon_{B4}$  such that the following holds. For each  $u, n$ , a set  $C_{u,n} \subset (1:U) \times (0:N)$  exists such that  $(\tilde{u}, \tilde{n}) \notin C_{u,n}$  implies  $B_{u,n}^+ \cap B_{\tilde{u},\tilde{n}}^+ = \emptyset$  and

$$\begin{aligned} & \left| g_{X_{B_{\tilde{u},\tilde{n}}}^P | X_{B_{u,n}}^P} - g_{X_{B_{\tilde{u},\tilde{n}}}^P | X_{B_{u,n}}^P} \right| < (1/2) \epsilon_{B4} g_{X_{B_{\tilde{u},\tilde{n}}}^P} g_{X_{B_{u,n}}^P} \\ & \left| g_{X_{B_{\tilde{u},\tilde{n}}}^P | \mathbf{X}_{0:N}} g_{X_{B_{u,n}}^P | \mathbf{X}_{0:N}} - g_{X_{B_{\tilde{u},\tilde{n}}}^P, X_{B_{u,n}}^P | \mathbf{X}_{0:N}} \right| \\ & < (1/2) \epsilon_{B4} g_{X_{B_{\tilde{u},\tilde{n}}}^P, X_{B_{u,n}}^P | \mathbf{X}_{0:N}} \end{aligned}$$

Further, there is a uniform bound  $|C_{u,n}| \leq c$ .

The mixing of the adapted process in Assumption B4 replaces the mixing of the unconditional process in Assumption A4. Though mixing of the adapted process may be hard to check, one may suspect that the adapted process typically mixes more rapidly than the unconditional process. Assumption B4 is needed only to ensure that the variance bound in Theorem 2 is essentially  $O(UN)$  rather than  $O(U^2N^2)$ . Either of these rates avoids the exponentially increasing variance

characterizing the curse of dimensionality. Lower variance than  $O(UN)$  cannot be anticipated for any sequential Monte Carlo method since the log likelihood estimate can be written as a sum of  $UN$  terms each of which involves its own sequential Monte Carlo calculation. The following Proposition S3 gives an implication of Assumption B4

**Proposition S3.** *Assumption B4 implies that, if  $(\tilde{u}, \tilde{n}) \notin C_{u,n}$ ,*

$$\text{Cov}_g(\gamma_{B_{u,n}}, \gamma_{B_{\tilde{u},\tilde{n}}}) < \epsilon_{B4} Q^{|B_{u,n}|+|B_{\tilde{u},\tilde{n}}|}. \quad (\text{S25})$$

*Proof.* Write  $\gamma = \gamma_{B_{u,n}}$  and  $\tilde{\gamma} = \gamma_{B_{\tilde{u},\tilde{n}}}$ . Also, write  $B = B_{u,n}$ ,  $\tilde{B} = B_{\tilde{u},\tilde{n}}$  and  $f_B(x_B^P) = f_{Y_B|X_B}(y_B^* | x_B^P)$ . Then,

$$\begin{aligned} \mathbb{E}[\gamma\tilde{\gamma}] &= \int \left[ \int f_B(x_B^P) g_{X_B^P|\mathbf{X}_{0:N}}(x_B^P | \mathbf{x}_{0:N}) dx_B^P \right] \\ &\quad \times \left[ \int f_{\tilde{B}}(x_{\tilde{B}}^P) g_{X_{\tilde{B}}^P|\mathbf{X}_{0:N}}(x_{\tilde{B}}^P | \mathbf{x}_{0:N}) dx_{\tilde{B}}^P \right] g_{\mathbf{X}_{0:N}}(\mathbf{x}_{0:N}) d\mathbf{x}_{0:N} \\ &= \int \int f_B(x_B^P) f_{\tilde{B}}(x_{\tilde{B}}^P) \left\{ \int g_{X_B^P|\mathbf{X}_{0:N}}(x_B^P | \mathbf{x}_{0:N}) \right. \\ &\quad \left. \times g_{X_{\tilde{B}}^P|\mathbf{X}_{0:N}}(x_{\tilde{B}}^P | \mathbf{x}_{0:N}) g_{\mathbf{X}_{0:N}}(\mathbf{x}_{0:N}) d\mathbf{x}_{0:N} \right\} dx_B^P dx_{\tilde{B}}^P \end{aligned} \quad (\text{S26})$$

Putting the approximate conditional independence requirement of Assumption B4 into (S26), we have

$$\begin{aligned} \left| \mathbb{E}[\gamma\tilde{\gamma}] - \int f_B(x_B^P) f_{\tilde{B}}(x_{\tilde{B}}^P) g_{X_B^P X_{\tilde{B}}^P|\mathbf{X}_{0:N}}(x_B^P, x_{\tilde{B}}^P | \mathbf{x}_{0:N}) g_{\mathbf{X}_{0:N}}(\mathbf{x}_{0:N}) dx_B^P dx_{\tilde{B}}^P d\mathbf{x}_{0:N} \right| \\ < (1/2) \epsilon_{B4} Q^{|B|+|\tilde{B}|}. \end{aligned}$$

This gives

$$\left| \mathbb{E}[\gamma\tilde{\gamma}] - \int f_B(x_B^P) f_{\tilde{B}}(x_{\tilde{B}}^P) g_{X_B^P X_{\tilde{B}}^P}(x_B^P, x_{\tilde{B}}^P) dx_B^P dx_{\tilde{B}}^P \right| < (1/2) \epsilon_{B4} Q^{|B|+|\tilde{B}|}. \quad (\text{S27})$$

Then, using the approximate unconditional independence requirement of Assumption B4 combined with the triangle inequality, (S27) implies

$$\left| \mathbb{E}[\gamma\tilde{\gamma}] - \int f_B(x_B^P) f_{\tilde{B}}(x_{\tilde{B}}^P) g_{X_B^P}(x_B^P) g_{X_{\tilde{B}}^P}(x_{\tilde{B}}^P) dx_B^P dx_{\tilde{B}}^P \right| < \epsilon_{B4} Q^{|B|+|\tilde{B}|}. \quad (\text{S28})$$

We can rewrite (S28) as

$$\left| \mathbb{E}[\gamma\tilde{\gamma}] - \mathbb{E}[\gamma] \mathbb{E}[\tilde{\gamma}] \right| < \epsilon_{B4} Q^{|B|+|\tilde{B}|}, \quad (\text{S29})$$

proving the proposition.  $\square$

**Assumption B5.** *There is a constant  $K$  such that, for any set  $D \subset (1:U) \times (n:n-d)$  and for all  $n \geq K + d$ ,  $\mathbf{x}_{n-d-K}^{(1)}$ ,  $\mathbf{x}_{n-d-K}^{(2)}$ , and all  $x_{D_n}$ ,*

$$\begin{aligned} \left| g_{X_D|\mathbf{X}_{n-d-K}}(x_D | \mathbf{x}_{n-d-K}^{(1)}) - g_{X_D|\mathbf{X}_{n-d-K}}(x_D | \mathbf{x}_{n-d-K}^{(2)}) \right| \\ < \epsilon_{B5} g_{X_D|\mathbf{X}_{n-d-K}}(x_{D_n} | \mathbf{x}_{n-d-K}^{(1)}) \end{aligned}$$

Assumption B5 is needed to ensure the stability of the Monte Carlo approximation to the adapted process. It ensures that any error due to finite Monte Carlo sample size has limited consequences at sufficiently remote time points. One could instead propose a bound that decreases exponentially with  $K$ , but that is not needed for the current purposes. The following Proposition S4 is useful for taking advantage of Assumption B5.

**Proposition S4.** *Suppose that  $f$  is a nonnegative function and that for some  $\epsilon > 0$ ,*

$$|f(x) - f(x')| < \epsilon f(x')$$

*holds for all  $x, x'$ . Then for any two probability distributions where the expectations are denoted by  $\mathbb{E}_1$  and  $\mathbb{E}_2$  and for any random variable  $X$ , we have*

$$|\mathbb{E}_1 f(X) - \mathbb{E}_2 f(X)| \leq \epsilon \mathbb{E}_2 f(X).$$

*Proof.* Let the two probability laws be denoted by  $P_1$  and  $P_2$ . We have

$$\begin{aligned} |\mathbb{E}_1 f(X) - \mathbb{E}_2 f(X)| &= \left| \int f(x) P_1(dx) - \int f(x') P_2(dx') \right| \\ &\leq \left| \int \int f(x) P_1(dx) P_2(dx') - \int \int f(x') P_1(dx) P_2(dx') \right| \\ &\leq \int \int |f(x) - f(x')| P_1(dx) P_2(dx') \\ &\leq \int \epsilon f(x') P_2(dx') = \epsilon \mathbb{E}_2 f(X). \end{aligned}$$

□

**Assumption B6.** *Let  $h$  be a bounded function with  $|h(x)| \leq 1$ . Let  $\mathbf{X}_{n,S,j,i}^{\text{IR}}$  be the Monte Carlo quantity constructed in ASIF-IR, conditional on  $\mathbf{X}_{n-1,S,i}^{\text{A}} = \mathbf{x}_{n-1,S,i}^{\text{A}}$ . There is a constant  $C_0(U, N, S)$  such that, for all  $\epsilon_{\text{B6}} > 0$  and  $\mathbf{x}_{n-1,S,i}^{\text{A}}$ , whenever the number of particles satisfies  $J > C_0(U, N, S)/\epsilon_{\text{B6}}^4$ ,*

$$\left| \mathbb{E} \left[ \frac{1}{J} \sum_{j=1}^J h(\mathbf{X}_{n,S,j,i}^{\text{IR}}) \right] - \mathbb{E}_g[h(\mathbf{X}_n) | \mathbf{X}_{n-1} = \mathbf{x}_{n-1,S,i}^{\text{A}}] \right| < \epsilon_{\text{B6}}.$$

Assumption B6 controls the Monte Carlo error for a single time interval on a single island. In the case  $S = 1$ , ASIF-IR becomes ASIF and this assumption is one of many alternatives for bounding error from importance sampling. The purpose behind the selection of Assumption B6 is to draw on the results of Park and Ionides (2019) for intermediate resampling, and our assumption is a restatement of their Theorem 2. When  $S = 1$ , the curse of dimensionality for importance sampling has the consequence that  $C_0$  grows exponentially with  $U$ . However, Park and Ionides (2019) showed that setting  $S = U$  can lead to situations where  $C_0(U, N, S)$  in Assumption B6 grows polynomially with  $U$ . Here, we do not place requirements concerning the dependence of  $C_0$  on  $U$ ,  $N$  and  $S$  since our immediate concern is a limit where  $\mathcal{I}$  and  $J$  increase. Nevertheless, the numerical results are consistent with the theoretical and empirical results obtained for intermediate resampling in the context of particle filtering by Park and Ionides (2019).

**Assumption B7.** For  $1 \leq n \leq N$ , the Monte Carlo random variable  $X_{n,i}^A$  is independent of  $w_{u,n,i,j}^M$  conditional on  $X_{n-1,i}^A$ .

The Monte Carlo conditional independence required by Assumption B7 would hold for ASIF-IR if the guide variance  $V_{u,n,i}$  were calculated using an independent set of guide simulations to those used for evaluating the measurement weights  $w_{u,n,i,j}^M$ . For numerical efficiency, the ASIF-IR algorithm implemented here constructs a shared pool of simulations for both purposes rather than splitting the pool up between them, in the expectation that the resulting minor violation of Assumption B7 has negligible impact.

**Theorem 2.** Let  $\ell^{MC}$  denote the Monte Carlo likelihood approximation constructed by ASIF-IR, or by ASIF since this is the special case of ASIF-IR with  $S = 1$ . Consider a limit with a growing number of islands,  $\mathcal{I} \rightarrow \infty$ , and suppose assumptions B1, B2, B3, B5, B6 and B7. Suppose the number of particles  $J$  exceeds the requirement for B6. There are quantities  $\epsilon(U, N)$  and  $V(U, N)$  with  $|\epsilon| < Q^2 \epsilon_{B1} + 2Q^{2b}(\epsilon_{B5} + (K + d_{u,n})\epsilon_{B6})$  and  $V < Q^{4b}U^2N^2$  such that

$$\mathcal{I}^{1/2}[\ell^{MC} - \ell - \epsilon UN] \xrightarrow[\mathcal{I} \rightarrow \infty]{d} \mathcal{N}[0, V]. \quad (\text{S30})$$

If additionally Assumption B4 holds, we obtain an improved rate of

$$V < Q^{4b}NU\{c + (\epsilon_{B4} + 3\epsilon_{B5} + 4(K + d_{\max})\epsilon_{B6})(NU - c)\} \quad (\text{S31})$$

*Proof.* First, we set up some notation. For  $B_{u,n}$  and  $w_{u,n,i,j}^M$  constructed by ASIF-IR, define

$$\gamma_{B_{u,n}}^{MC,i} = \prod_{m=1}^n \left[ \frac{1}{J} \sum_{j=1}^J \prod_{(\tilde{u},m) \in B_{u,n}^{[m]}} w_{\tilde{u},m,i,j}^M \right] \quad \text{and} \quad \bar{\gamma}_{B_{u,n}}^{MC} = \frac{1}{\mathcal{I}} \sum_{i=1}^{\mathcal{I}} \gamma_{B_{u,n}}^{MC,i}. \quad (\text{S32})$$

The Monte Carlo conditional likelihoods output by ASIF-IR can be written as

$$\ell_{u,n}^{MC} = \log \bar{\gamma}_{B_{u,n}^+}^{MC} - \log \bar{\gamma}_{B_{u,n}}^{MC}. \quad (\text{S33})$$

We proceed with a similar argument to the proof of Theorem 1. Since  $\gamma_{B_{u,n}}^{MC,i}$  are i.i.d. for  $i \in 1:\mathcal{I}$ , we can suppose they are replicates of a Monte Carlo random variable  $\gamma_{B_{u,n}}^{MC}$ . We define

$$\Delta_{u,n}^+ = \frac{1}{\sqrt{\mathcal{I}}} \sum_{i=1}^{\mathcal{I}} (\gamma_{B_{u,n}^+}^{MC,i} - \mathbb{E}[\gamma_{B_{u,n}^+}^{MC}]), \quad \Delta_{u,n} = \frac{1}{\sqrt{\mathcal{I}}} \sum_{i=1}^{\mathcal{I}} (\gamma_{B_{u,n}}^{MC,i} - \mathbb{E}[\gamma_{B_{u,n}}^{MC}]).$$

The same calculation as (S13) gives

$$\ell_{u,n}^{MC} = \log \left( \frac{\mathbb{E}[\gamma_{B_{u,n}^+}^{MC}]}{\mathbb{E}[\gamma_{B_{u,n}}^{MC}]} \right) + \mathcal{I}^{-1/2} \left( \frac{\Delta_{u,n}^+}{\mathbb{E}[\gamma_{B_{u,n}^+}^{MC}]} - \frac{\Delta_{u,n}}{\mathbb{E}[\gamma_{B_{u,n}}^{MC}]} \right) + o_P(\mathcal{I}^{-1/2}) \quad (\text{S34})$$

The joint distribution of  $\{(\Delta_{u,n}^+, \Delta_{u,n}), (u, n) \in 1:U \times 1:N\}$  follows a standard central limit theorem as  $\mathcal{I} \rightarrow \infty$ . Each term has mean zero, with variances and covariances uniformly bounded over  $(u, n, \tilde{u}, \tilde{n})$  due to Assumption B3. From Proposition S2, using the same reasoning as (S18),

$$\left| \log \left( \frac{\mathbb{E}_g[\gamma_{A_{u,n}^+}]}{\mathbb{E}_g[\gamma_{A_{u,n}}]} \right) - \log \left( \frac{\mathbb{E}_g[\gamma_{B_{u,n}^+}]}{\mathbb{E}_g[\gamma_{B_{u,n}}]} \right) \right| < \epsilon_{B1}Q^2. \quad (\text{S35})$$

Now we use Lemma S2 and (S17) to obtain

$$\begin{aligned}
& \left| \log \left( \frac{\mathbb{E}_g[\gamma_{B_{u,n}^+}]}{\mathbb{E}_g[\gamma_{B_{u,n}}]} \right) - \log \left( \frac{\mathbb{E}[\gamma_{B_{\tilde{u},\tilde{n}}^{MC}}]}{\mathbb{E}[\gamma_{B_{u,n}}]} \right) \right| \\
& \leq \left| \log \mathbb{E}_g[\gamma_{B_{u,n}^+}] - \log \mathbb{E}[\gamma_{B_{u,n}^+}] \right| + \left| \log \mathbb{E}_g[\gamma_{B_{u,n}}] - \log \mathbb{E}[\gamma_{B_{u,n}}] \right| \\
& < 2Q^{2b}(\epsilon_{B5} + (K + d_{\max})\epsilon_{B6}). \tag{S36}
\end{aligned}$$

The proof of the central limit result in (S30) is completed by combining (S34), (S35) and (S36). To show (S31) we check that  $\Delta_{u,n}$  and  $\Delta_{\tilde{u},\tilde{n}}$  are weakly correlated when  $(u, n)$  and  $(\tilde{u}, \tilde{n})$  are sufficiently separated. By the same reasoning as the proof of Theorem 1, it is sufficient to show that  $\gamma_{B_{u,n}}^{MC}$  and  $\gamma_{B_{\tilde{u},\tilde{n}}}^{MC}$  are weakly correlated. These Monte Carlo quantities approximate  $\gamma_{B_{u,n}}(\mathbf{X}_{0:n-1})$  and  $\gamma_{B_{\tilde{u},\tilde{n}}}(\mathbf{X}_{0:\tilde{n}-1})$  with  $\mathbf{X}$  drawn from  $g$ . Let us suppose  $n \geq \tilde{n}$ , and write  $d_{u,n} = n - \inf_{(v,m) \in B_{u,n}} m$ . First, we consider the situation  $n - \tilde{n} > K + d_{u,n}$ , in which case we can use the Markov property to give

$$\text{Cov}(\gamma_{B_{u,n}}^{MC}, \gamma_{B_{\tilde{u},\tilde{n}}}^{MC}) < \mathbb{E}[\gamma_{B_{\tilde{u},\tilde{n}}}^{MC}] \sup_{\mathbf{x}} \left\{ \mathbb{E}[\gamma_{B_{u,n}}^{MC} | \mathbf{X}_{n-d_{u,n}-K,1}^A = \mathbf{x}] - \mathbb{E}[\gamma_{B_{u,n}}^{MC}] \right\} \tag{S37}$$

Then, the triangle inequality followed by applications of Assumption B5 and Lemma S2 gives

$$\begin{aligned}
& \left| \mathbb{E}[\gamma_{B_{u,n}}^{MC} | \mathbf{X}_{n-d_{u,n}-K,1}^A = \mathbf{x}] - \mathbb{E}[\gamma_{B_{u,n}}^{MC}] \right| \\
& \leq \left| \mathbb{E}_g[\gamma_{B_{u,n}} | \mathbf{X}_{n-d_{u,n}-K} = \mathbf{x}] - \mathbb{E}_g[\gamma_{B_{u,n}}] \right| \\
& \quad + \left| \mathbb{E}[\gamma_{B_{u,n}}^{MC} | \mathbf{X}_{n-d_{u,n}-K,1}^A = \mathbf{x}] - \mathbb{E}_g[\gamma_{B_{u,n}} | \mathbf{X}_{n-d_{u,n}-K} = \mathbf{x}] \right| \\
& \quad + \left| \mathbb{E}[\gamma_{B_{u,n}}^{MC}] - \mathbb{E}_g[\gamma_{B_{u,n}}] \right| \\
& \leq Q^b \left( 2\epsilon_{B5} + 2(K + d_{u,n})\epsilon_{B6} \right) \tag{S38}
\end{aligned}$$

Putting (S38) into (S37), we get

$$\text{Cov}(\gamma_{B_{u,n}}^{MC}, \gamma_{B_{\tilde{u},\tilde{n}}}^{MC}) < Q^{2b} \left( 2\epsilon_{B5} + 2(K + d_{u,n})\epsilon_{B6} \right). \tag{S39}$$

Now we address the situation  $n - \tilde{n} \leq K + d_{u,n}$ . We apply Lemma S2 on the union  $B_{u,n} \cup B_{\tilde{u},\tilde{n}}$  for which the temporal depth is bounded by  $d \leq K + d_{u,n} + d_{\tilde{u},\tilde{n}}$ . This gives

$$\left| \mathbb{E}[\gamma_{B_{u,n}}^{MC} \gamma_{B_{\tilde{u},\tilde{n}}}^{MC}] - \mathbb{E}_g[\gamma_{B_{u,n}} \gamma_{B_{\tilde{u},\tilde{n}}}] \right| < Q^{2b} \left( (2K + d_{u,n} + d_{\tilde{u},\tilde{n}})\epsilon_{B6} + \epsilon_{B5} \right). \tag{S40}$$

From Proposition S3, if  $(\tilde{u}, \tilde{n}) \notin C_{u,n}$ ,

$$\text{Cov}_g(\gamma_{B_{u,n}}, \gamma_{B_{\tilde{u},\tilde{n}}}) < \epsilon_{B4} Q^{2b}. \tag{S41}$$

Now, we establish that  $\text{Cov}(\gamma_{B_{u,n}}^{MC}, \gamma_{B_{\tilde{u},\tilde{n}}}^{MC})$  is close to  $\text{Cov}_g(\gamma_{B_{u,n}}, \gamma_{B_{\tilde{u},\tilde{n}}})$ .

$$\begin{aligned}
& \left| \text{Cov}(\gamma_{B_{u,n}}^{MC}, \gamma_{B_{\tilde{u},\tilde{n}}}^{MC}) - \text{Cov}_g(\gamma_{B_{u,n}}, \gamma_{B_{\tilde{u},\tilde{n}}}) \right| \\
& \leq \left| \mathbb{E}[\gamma_{B_{u,n}}^{MC} \gamma_{B_{\tilde{u},\tilde{n}}}^{MC}] - \mathbb{E}_g[\gamma_{B_{u,n}} \gamma_{B_{\tilde{u},\tilde{n}}}] \right| \\
& \quad + \left| \mathbb{E}[\gamma_{B_{u,n}}^{MC}] (\mathbb{E}[\gamma_{B_{\tilde{u},\tilde{n}}}^{MC}] - \mathbb{E}_g[\gamma_{B_{\tilde{u},\tilde{n}}})) \right| \\
& \quad + \left| \mathbb{E}[\gamma_{B_{\tilde{u},\tilde{n}}}^{MC}] (\mathbb{E}[\gamma_{B_{u,n}}^{MC}] - \mathbb{E}_g[\gamma_{B_{u,n}}]) \right| \\
& < Q^{2b} \left( (2K + d_{u,n} + d_{\tilde{u},\tilde{n}}) \epsilon_{B6} + \epsilon_{B5} + 2(\epsilon_{B5} + (K + d_{\max}) \epsilon_{B6}) \right). \\
& < Q^{2b} \left( 3\epsilon_{B5} + 4(K + d_{\max}) \epsilon_{B6} \right) \tag{S42}
\end{aligned}$$

Using (S42) together with (S41) to bound the  $UN(UN - c)$  off-diagonal covariance terms completes the derivation of (S31).  $\square$

**Lemma S2.** *Suppose Assumptions B3, B5, B6 and B7. Suppose the number of particles  $J$  exceeds the requirement for B6. If we write  $d_B = \max_{(u_1, n_1), (u_2, n_2) \in B} |n_1 - n_2|$  for  $B \subset 1:U \times 1:N$ , then for any  $B$ ,*

$$\left| \mathbb{E}[\gamma_B^{MC} | \mathbf{X}_{n-d_B-K,1}^A = \mathbf{x}] - \mathbb{E}_g[\gamma_B | \mathbf{X}_{n-d_B-K} = \mathbf{x}] \right| < Q^{|B|} (K + d_B) \epsilon_{B6}, \quad \forall \mathbf{x} \in \mathbb{X}^U,$$

and

$$\left| \mathbb{E}[\gamma_B^{MC}] - \mathbb{E}_g[\gamma_B] \right| < Q^{|B|} (\epsilon_{B5} + (K + d_B) \epsilon_{B6}). \tag{S43}$$

*Proof.* Suppose that  $\max_{(u', n') \in B} n' = n$ . Define  $\eta_n(\mathbf{x}_n) = 1$  and, for  $0 \leq m \leq n - 1$ ,

$$\eta_m(\mathbf{x}_m) = \mathbb{E}_g \left[ \prod_{k=m+1}^n \gamma_{B^{[k]}} \mid \mathbf{X}_m = \mathbf{x}_m \right]. \tag{S44}$$

We have a recursive identity

$$\eta_m(\mathbf{X}_m) = \mathbb{E}_g \left[ \gamma_{B^{[m+1]}} \eta_{m+1}(\mathbf{X}_{m+1}) \mid \mathbf{X}_m \right]. \tag{S45}$$

By taking the expectation of (S44), we have

$$\mathbb{E}_g[\eta_0(\mathbf{X}_0)] = \mathbb{E}_g[\gamma_B]. \tag{S46}$$

Note that  $g$  has marginal density  $f_{\mathbf{X}_0}$  for  $\mathbf{X}_0$ . We analyze an ASIF-IR approximation to (S45). The function  $\eta_{m+1}(\mathbf{x})$  is not in practice computationally available for evaluation via ASIF-IR, but the recursion nevertheless leads to a useful bound. Let  $\mathbf{X}_{m+1}^A[j](\mathbf{x}_m)$  correspond to the variable  $\mathbf{X}_{m+1, S, 1, j}^{IR}$  constructed by ASIF-IR conditional on  $\mathbf{X}_{m, 1}^A = \mathbf{x}_m$ . Equivalently,  $\mathbf{X}_{m+1}^A[j](\mathbf{x}_m)$  matches the variable  $\mathbf{X}_{m+1, 1}^A$  in ASIF-IR if the assignment  $\mathbf{X}_{m+1, 1}^A = \mathbf{X}_{m+1, S, 1, 1}^{IR}$  is replaced by  $\mathbf{X}_{m+1, 1}^A = \mathbf{X}_{m+1, S, 1, j}^{IR}$  conditional on  $\mathbf{X}_{m, 1}^A = \mathbf{x}_m$ . We define an approximation error  $e_m(\mathbf{x}_m)$  by

$$\eta_m(\mathbf{x}_m) = \frac{1}{J} \sum_{j=1}^J f_{Y_{B^{[m+1]}} | \mathbf{X}_m}(y_{B^{[m+1]}}^* | \mathbf{x}_m) \eta_{m+1}(\mathbf{X}_{m+1}^A[j](\mathbf{x}_m)) + e_m(\mathbf{x}_m). \tag{S47}$$

From Assumptions B3 and B6,  $\mathbb{E}|e_m(\mathbf{x}_m)| < \epsilon_{B6} Q^{|B^{[m+1:n]}|}$  uniformly over  $\mathbf{x}_m$ , Thus, setting  $r_m = \mathbb{E}|e_m(\mathbf{X}_{m,1}^A)|$ , we have

$$r_m < \epsilon_{B6} Q^{|B^{[m+1:n]}|}. \quad (\text{S48})$$

Now, setting  $K' = K + d_{u,n}$ , we commence to prove inductively that, for  $n - K' \leq m \leq n$ ,

$$\left| \eta_{n-K'}(\mathbf{x}) - \mathbb{E} \left[ \eta_m(\mathbf{X}_{m,1}^A) \prod_{k=n-K'+1}^m f_{Y_{B^{[k]}|\mathbf{X}_{k-1}}}(y_{B^{[k]}}^* | \mathbf{X}_{k-1,1}^A) \middle| \mathbf{X}_{n-K',1}^A = \mathbf{x} \right] \right| < (m-n+K')\epsilon_{B6} Q^{|B|}. \quad (\text{S49})$$

First, suppose that (S49) holds for  $m$ . From (S47) and (S48),

$$\left| \eta_m(\mathbf{x}_m) - \mathbb{E} \left[ \frac{1}{J} \sum_{j=1}^J f_{Y_{B^{[m+1]}|\mathbf{X}_m}}(y_{B^{[m+1]}}^* | \mathbf{x}_m) \eta_{m+1}(\mathbf{X}_{m+1}^A[j](\mathbf{x}_m)) \right] \right| < \epsilon_{B6} Q^{|B^{[m+1:n]}|}. \quad (\text{S50})$$

Since the particles are exchangeable, the expectation of the mean of  $J$  particles can be replaced with the expectation of the first particle. Plugging in  $\mathbf{x}_m = \mathbf{X}_{m,1}^A$  gives us

$$\left| \eta_m(\mathbf{X}_{m,1}^A) - f_{Y_{B^{[m+1]}|\mathbf{X}_m}}(y_{B^{[m+1]}}^* | \mathbf{X}_{m,1}^A) \mathbb{E} [\eta_{m+1}(\mathbf{X}_{m+1,1}^A) | \mathbf{X}_{m,1}^A] \right| < \epsilon_{B6} Q^{|B^{[m+1:n]}|} \quad (\text{S51})$$

Putting (S51) into (S49), for  $m \leq n$ , and taking an iterated expectation with respect to  $\mathbf{X}_{m,1}^A$ , we find that (S49) holds also for  $m+1$ . Since (S49) holds trivially for  $m = n - K'$ , it holds for  $n - K' \leq m \leq n$  by induction. Then, noting  $\eta_n(\mathbf{x}) = 1$ , we have from (S49) that

$$\left| \eta_{n-K'}(x) - \mathbb{E} \left[ \prod_{k=n-K'+1}^n f_{Y_{B^{[k]}|\mathbf{X}_{k-1}}}(y_{B^{[k]}}^* | \mathbf{X}_{k-1,1}^A) \middle| \mathbf{X}_{n-K',1}^A = x \right] \right| < K' \epsilon_{B6} Q^{|B|}.$$

Integrating the above inequality over  $\mathbf{x}$  with respect to the law of  $\mathbf{X}_{n-K',1}^A$ , we obtain

$$\left| \mathbb{E}[\eta_{n-K'}(\mathbf{X}_{n-K',1}^A)] - \mathbb{E} \left[ \prod_{k=n-K'+1}^n f_{Y_{B^{[k]}|\mathbf{X}_{k-1}}}(y_{B^{[k]}}^* | \mathbf{X}_{k-1,1}^A) \right] \right| < K' \epsilon_{B6} Q^{|B|}. \quad (\text{S52})$$

But under Assumption B7, we have

$$\mathbb{E} \left[ \prod_{k=n-K'+1}^n f_{Y_{B^{[k]}|\mathbf{X}_{k-1}}}(y_{B^{[k]}}^* | \mathbf{X}_{k-1,1}^A) \right] = \mathbb{E}[\gamma_B^{MC}]. \quad (\text{S53})$$

Assumption B5 says

$$|\eta_{n-K'}(\mathbf{x}_{n-K'}^{(1)}) - \eta_{n-K'}(\mathbf{x}_{n-K'}^{(2)})| < \epsilon_{B5} \eta_{n-K'}(\mathbf{x}_{n-K'}^{(2)}). \quad (\text{S54})$$

Application of Proposition S4 to (S54) gives

$$\left| \mathbb{E}_g[\eta_{n-K'}(\mathbf{X}_{n-K'})] - \mathbb{E}[\eta_{n-K'}(\mathbf{X}_{n-K',1}^A)] \right| < \epsilon_{B5} \mathbb{E}_g[\eta_{n-K'}(\mathbf{X}_{n-K'})] < \epsilon_{B5} Q^{|B|}. \quad (\text{S55})$$

Combining (S52), (S53), and (S55) completes the proof of Lemma S2.  $\square$

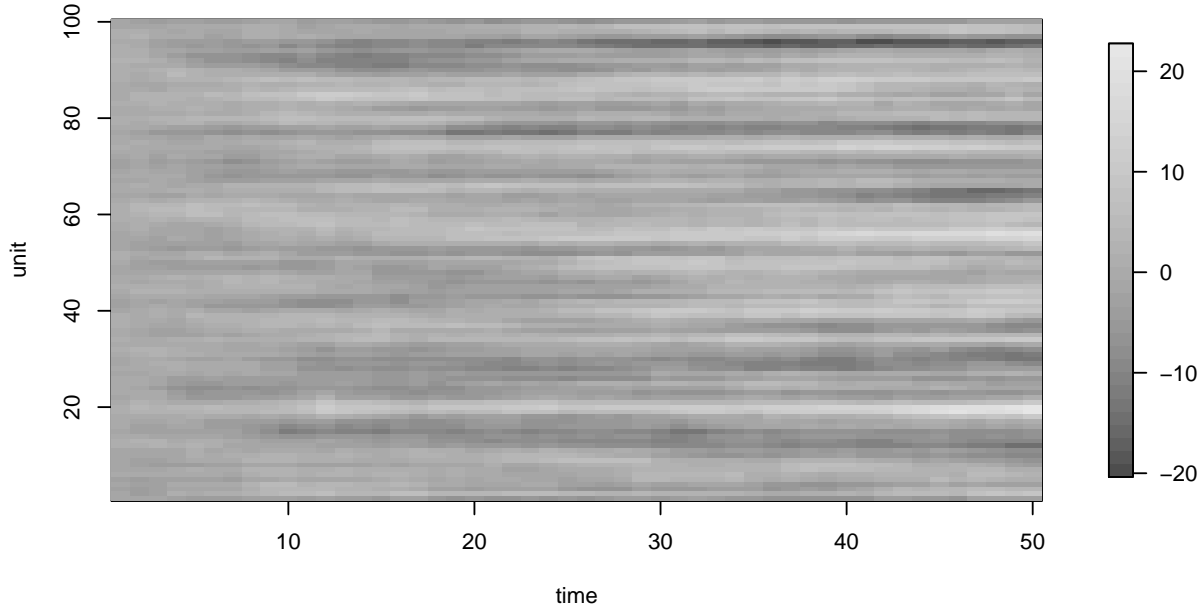


Figure S-1: correlated Brownian motion simulation used in the main text

## S5 The correlated Brownian motion example

To help visualize the correlated Brownian motion model, Fig. S-1 shows one of the simulations used for the results in Figure 3 of the main text. Table S-1 gives the algorithmic settings used for the filters and corresponding computational resource requirements. Broadly speaking,  $\mathcal{IJ}$  for ASIF and ASIF-IR should be compared with  $\mathcal{I}$  for BIF,  $J$  for PF, and  $JG$  for GIRF.

The computational effort allocated to each algorithm in Table S-1 is given in core minutes. BIF, ASIF and ASIF-IR parallelize readily, which is less true for PF and GIRF. Therefore, the BIF, ASIF and ASIF-IR implementations run on all available cores (40 for this experiment) whereas the PF and GIRF implementations run on a single core. If sufficient replications are being carried out to utilize all available cores, comparison of core minute utilization is equivalent to comparison of total computation time. However, a single replication of BIF, ASIF or ASIF-IR proceeds more quickly due to the parallelization.



	BIF	ASIF	ASIF-IR	GIRF	PF
particles, $J$	—	400	200	1000	100000
islands, $\mathcal{I}$	40000	400	200	—	—
guide simulations, $G$	—	—	—	50	—
lookahead lag, $L$	—	—	—	2	—
intermediate steps, $S$	—	—	$U/2$	$U$	—
neighborhood, $B_{u,n}$	$\{(u-1,n),(u-2,n),$ $(u,n-1),(u,n-2)\}$			—	—
forecast mean, $\boldsymbol{\mu}(\boldsymbol{x}, s, t)$	—	—	$\boldsymbol{x}$		—
measurement mean, $h_{u,n}(x)$	—	—	$x$		—
$\tau = \overleftarrow{v}_{u,n}(V, x)$	—	—	$\sqrt{V}$		—
$V = \overrightarrow{v}_{u,n}(\tau, x)$	—	—	$\tau^2$		—
effort (core mins, $U = 5$ )	2.5	4.7	6.6	0.6	0.6
effort (core mins, $U = 10$ )	4.3	7.8	14.0	1.3	1.1
effort (core mins, $U = 20$ )	8.0	14.1	40.8	3.4	2.3
effort (core mins, $U = 40$ )	15.6	28.5	169.0	10.2	5.0
effort (core mins, $U = 80$ )	30.6	60.6	886.0	42.5	12.3

Table S-1: Algorithmic settings for the correlated Brownian motion numerical example. Computational effort is measured in core minutes for running one filter, corresponding to a point on Figure 1 in the main text. The time taken for computing a single point using the parallel BIF, ASIF and ASIF-IR implementations is the effort divided by the number of cores, here 40. The time taken for computing a single point using the serial GIRF and PF implementations is equal to the effort in core minutes.

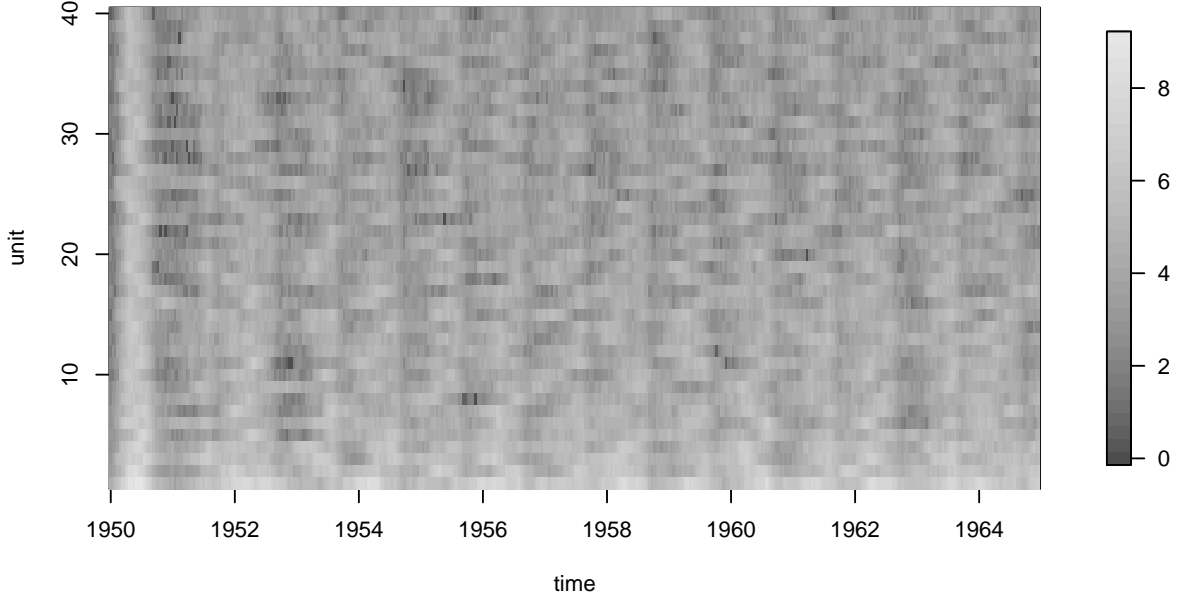


Figure S-2:  $\text{Log}_{10}$  (reported cases + 1) for the measles simulation used in the main text.

## S6 The measles example

Fig. S-2 shows the simulation used for the measles scaling experiment in Figure 2 and the likelihood slice shown in Figure 3 of the main text. Unit  $u$  models the  $u$ th largest city in UK. Table S-2 gives the model parameter values and Table S-3 gives the algorithmic settings used for the filters. The times in Table S-3 give the total time required by each algorithm to calculate all its results for Figure 2 in the main text, using 30 cores. The expected forecast function  $\mu(x, s, t)$  needed for ASIF-IR and GIRF was computed using a numerical solution to the deterministic skeleton of the stochastic model, i.e, a system of ODEs with derivative matching the infinitesimal mean function of the stochastic dynamic model. In the specifications of  $h_u(x)$ ,  $\overleftarrow{v}_u(V, x, \theta)$  and  $\overrightarrow{v}_u(\theta, x)$ , the latent process value  $x$  contains a variable  $C$  giving the cumulative removed infections in the current observation interval.

In Table S-3, we see that the effort allocated to BIF, ASIF and PF scales linearly with  $U$ , since the number of particles and islands is fixed in this experiment. GIRF computational effort scales fairly linearly in  $U$ , since its effort is dominated by the guide simulations (which are linear in  $U$ ) rather than by the intermediate timestep calculations (which are quadratic in  $U$  since we carry out  $U$  intermediate calculations each of size linear in  $U$ ). The effort allocated to ASIF-IR scales with  $U^2$ , since ASIF-IR is more parsimonious with guide simulations (all particles on an island share the same guide simulations) and so the intermediate timestep calculations dominate the effort. To obtain stable variance in the log likelihood estimate, the number of particles and islands would have to grow with  $U$ . However, given a constraint on total computational resources, the number of particles and islands would have to shrink as  $U$  increases. The limit studied in this experiment is a balance between the two: the assumption is that one is prepared to invest a growing amount of computational effort as the data grow, but this should not grow too fast. ASIF-IR was permitted

parameter	value	unit	description
$\bar{\beta}$	1727.9	year <sup>-1</sup>	mean contact rate
$\mu_{\bullet D}^{-1}$	50.0	year	mean duration in the population
$\mu_{EI}^{-1}$	12.6	day	latent period
$\mu_{IR}^{-1}$	12.0	day	infectious period
$\sigma_{SE}$	0.088	year <sup>1/2</sup>	process noise
$a$	0.554	—	amplitude of seasonality
$\alpha$	0.976	—	mixing exponent
$\tau$	4	year	delay from birth to entry into susceptibles
$\rho$	0.488	—	reporting probability
$\psi$	0.116	—	reporting overdispersion
$G$	150	—	gravitation constant

Table S-2: Table of parameters for the spatiotemporal measles transmission model

the greatest computational effort, but two considerations balance this.

1. Parallelization. BIF, ASIF and ASIF-IR are trivially parallelizable. The value of parallelization depends, among other things, on how many replications are being computed simultaneously and on how many cores are available. Nevertheless, it is helpful that the core minute effort requirement for ASIF and ASIF-IR can be divided by the number of available cores to give the computational time. Parallelizations of GIRF and PF can be constructed (Park and Ionides; 2019) but these involve non-trivial interaction between processors leading to additional algorithmic complexity and computational overhead.
2. Memory. The intermediate timestep calculations in ASIF-IR and GIRF do not add to the memory requirement, and the memory demands of BIF, ASIF and ASIF-IR are distributed across the parallel computations. A basic PF implementation for a large model can become constrained by its memory requirement (linear in the number of particles) before it can match the processor effort employed by the other algorithms.

	BIF	ASIF	ASIF-IR	GIRF	PF
particles, $J$	1	500	200	2000	100000
islands, $\mathcal{I}$	40000	500	200	—	—
guide simulations, $G$	—	—	—	40	—
lookahead lag, $L$	—	—	—	1	—
intermediate steps, $S$	—	—	$U/2$	$U$	—
neighborhood, $B_{u,n}$	$\{(u, n - 1), (u, n - 2)\}$			—	—
forecast mean, $\boldsymbol{\mu}(\boldsymbol{x}, s, t)$	—	—	ODE model		—
measurement mean, $h_{u,n}(x)$	—	—	$\rho C$		—
$\psi = \overleftarrow{v}_{u,n}(V, x)$	—	—	$\frac{\sqrt{V - \rho(1 - \rho)C}}{\rho C}$		—
$V = \overrightarrow{v}_{u,n}(\psi, \rho, x)$	—	—	$\rho(1 - \rho)C + \rho^2 C^2 \psi^2$		—
effort (core mins, $U = 2$ )	57.8	11.8	6.5	1.9	2.3
effort (core mins, $U = 4$ )	91.1	19.7	16.2	4.2	4.4
effort (core mins, $U = 8$ )	154.1	36.4	56.3	13.7	11.3
effort (core mins, $U = 16$ )	286.6	71.0	236.4	35.4	20.3
effort (core mins, $U = 32$ )	555.2	139.5	1054.9	100.6	34.8

Table S-3: Algorithmic settings for the measles example calculations in Figures 2 and 3. Computational effort is measured in core minutes for running one filter, corresponding to a point on Figure 2. The time taken for computing a single point using the parallel BIF, ASIF and ASIF-IR implementations is the effort divided by the number of cores, here 40. The time taken for computing a single point using the serial GIRF and PF implementations is equal to the effort in core minutes.

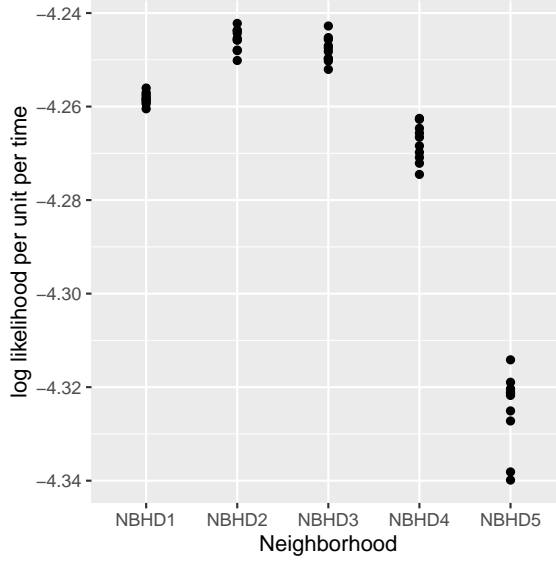


Figure S-3: log likelihood estimates for simulated data from the measles model using ASIF, with varying neighborhoods.

## S7 Varying the neighborhood for measles

We compared five different neighborhoods for the measles model:

NBHD1	One co-located lag	$\{(u, n - 1)\}$
NBHD2	Two co-located lags	$\{(u, n - 1), (u, n - 2)\}$
NBHD3	Three co-located lags	$\{(u, n - 1), (u, n - 2), (u, n - 3)\}$
NBHD4	Two co-located lags and the previous city	$\{(u, n - 1), (u, n - 2), (u - 1, n)\}$
NBHD5	Two co-located lags and London	$\{(u, n - 1), (u, n - 2), (1, n)\}$

We filtered simulated data for  $U = 40$  and  $N = 104$ , with 10 replications. We used ASIF with 1000 particles on each of 1000 islands. The results are shown in Figure S-3. Larger neighborhoods should increase the expected likelihood, but their increased Monte Carlo variability can decrease the expected log likelihood due to Jensen’s inequality. In this case, we see that a neighborhood of two co-located lags provides a reasonable bias-variance tradeoff.

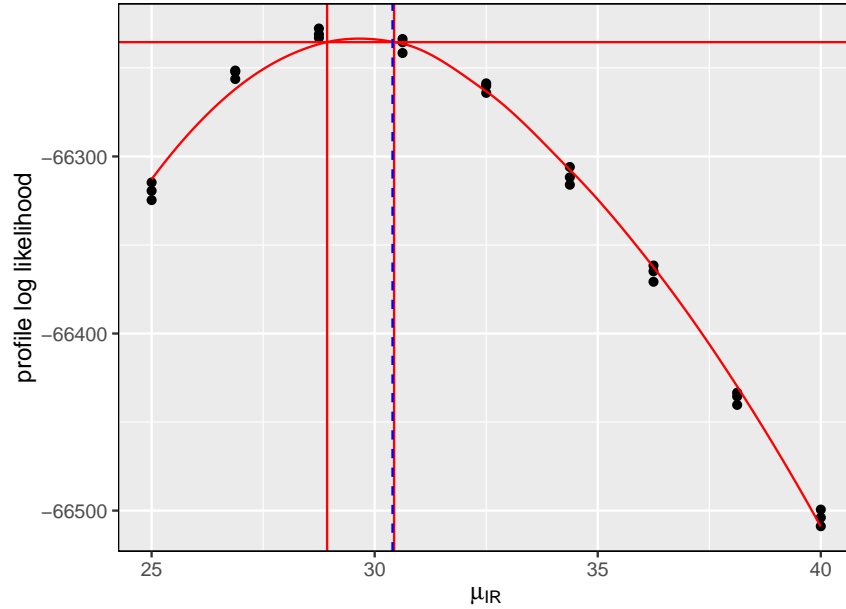


Figure S-4: Likelihood slice of the recovery rate parameter, computed via ASIF on the measles model with  $U = 40$  cities. Data were simulated using a parameter value of 30.4 (blue dashed line). ASIF is run three times for every parameter slice value.

## S8 A likelihood slice across recovery rate for the measles model

As discussed in the main text, we expect parameters of within-city transmission that are shared between cities to be well identified. Figure S-4 shows a likelihood slice for the per-capita recovery rate,  $\mu_{IR}$  (in units of  $\text{year}^{-1}$ ) on simulated data from the coupled model for  $U = 40$  cities. As expected, the likelihood has peak in the vicinity of the truth at  $\mu_{IR} = 30.4 \text{ year}^{-1}$ . The rapid decrease in the log likelihood away from this maximum dwarfs the Monte Carlo error in computing this log likelihood.

## S9 A Lorenz '96 example

Our primary motivation for ASIF and ASIF-IR is application to population dynamics arising in ecological and epidemiological models. Geophysical models provide an alternative situation involving spatiotemporal data analysis. We compare methods on the Lorenz '96 model, a nonlinear chaotic system providing a toy model for global atmospheric circulation (Lorenz; 1996). We consider a stochastic Lorenz '96 model with added Gaussian process noise (Park and Ionides; 2019) defined as the solution to the following system of stochastic differential equations,

$$dX_u(t) = \{(X_{u+1}(t) - X_{u-2}(t)) \cdot X_{u-1}(t) - X_u(t) + F\}dt + \sigma_p dB_u(t), \quad u \in 1:U. \quad (\text{S56})$$

We define  $X_0 = X_U$ ,  $X_{-1} = X_{U-1}$ , and  $X_{U+1} = X_1$  so that the  $U$  spatial locations are placed on a circle. The terms  $\{B_u(t), u \in 1:U\}$  denote  $U$  independent standard Brownian motions.  $F$  is a forcing constant, and we use the value  $F = 8$  which was demonstrated by Lorenz (1996) to induce chaotic behavior. The process noise parameter is set to  $\sigma_p = 1$ . The system is started at the initial state  $X_u(0) = 0$  for  $u \in 1:U$ . Observations are independently made for each dimension at  $t_n = n$  for  $n \in 1:N$  with Gaussian measurement noise of mean zero and standard deviation  $\tau = 1$ ,

$$Y_{u,n} = X_u(t_n) + \eta_{u,n} \quad \eta_{u,n} \sim N(0, \tau^2). \quad (\text{S57})$$

We used an Euler-Maruyama method for numerical approximation of the sample paths of  $\{\mathbf{X}(t)\}$ , with timestep of 0.01. A simulation from this model is shown in Fig. S-6.

The ensemble Kalman filter (EnKF) is a widely used filtering method in weather forecasting for high dimensional systems (Evensen and van Leeuwen; 1996). EnKF involves a local Gaussian approximation which is problematic in highly nonlinear systems (Ades and Van Leeuwen; 2015). Methods that make local Gaussian assumptions like EnKF are necessary to scale up to the dimensions of the problems in weather forecasting. Figure S-5 shows that for a small number of units, the basic particle filter (PF) and GIRF out-perform EnKF. Then, as the number of spatial units increases, the performance of PF rapidly deteriorates whereas GIRF continues to perform well up to a moderate number of units. BIF, ASIF, and particularly ASIFIR, scales well despite underperforming EnKF on this example. The additive Gaussian observation and process noise in the Lorenz '96 model is well suited to the approximations involved in EnKF. By contrast, it is less clear how to apply EnKF to discrete population non-Gaussian models such as the measles example, and how effective the resulting approximations might be.

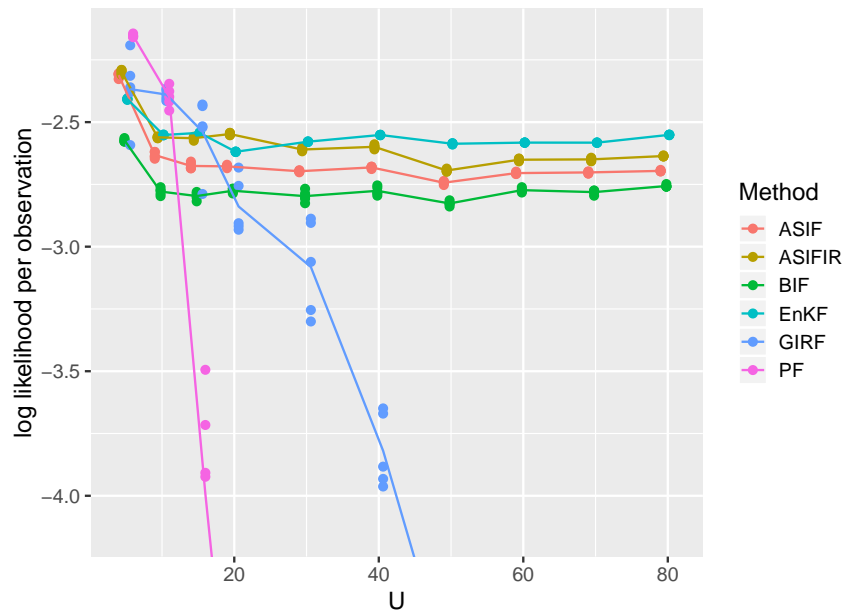


Figure S-5: Log likelihood estimates for a Lorenz '96 model of various dimensions. BIF, ASIF and ASIF-IR are compared with a guided intermediate resampling filter (GIRF), a basic particle filter (PF) and an ensemble Kalman filter (EnKF).

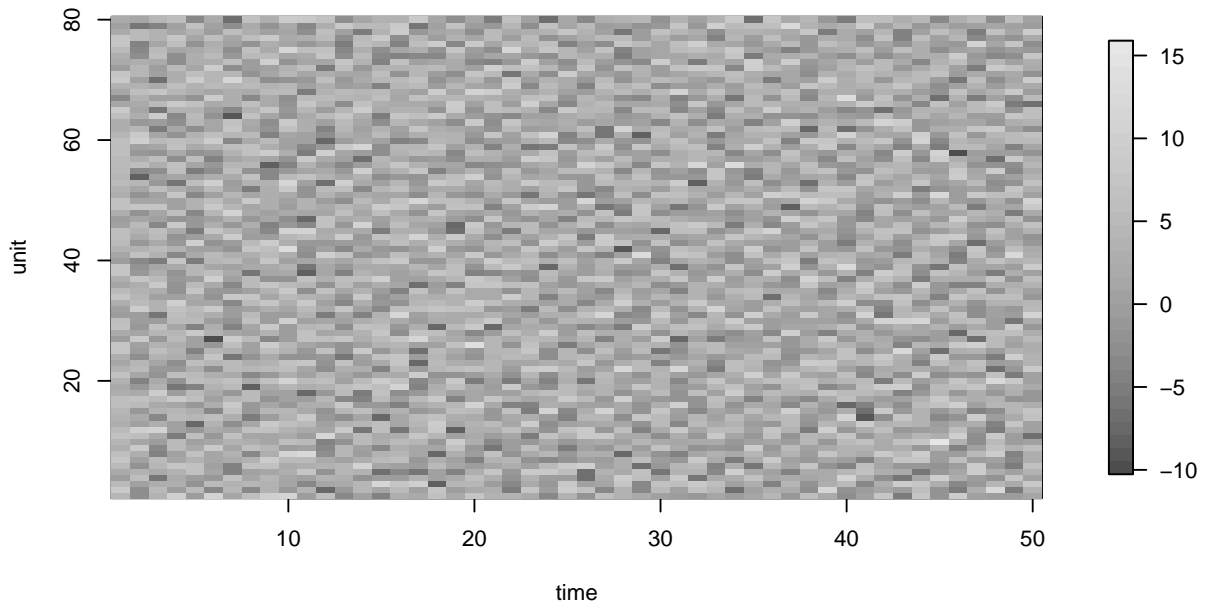


Figure S-6: Lorenz '96 simulation used in the main text



	BIF	ASIF	ASIF-IR	GIRF	PF	EnKF
particles, $J$	1	400	200	1000	100000	10000
islands, $\mathcal{I}$	40000	400	200	—	—	—
guide simulations, $G$	—	—	—	50	—	—
lookahead lag, $L$	—	—	—	2	—	—
intermediate steps, $S$	—	—	$U/2$	$U$	—	—
neighborhood, $B_{u,n}$	$\{(u,n-1),(u,n-2),$ $(u-1,n),(u-2,n)\}$			—	—	—
forecast mean, $\boldsymbol{\mu}(\boldsymbol{x}, s, t)$	—	—	ODE model		—	—
measurement mean, $h_{u,n}(x)$	—	—	$x$		—	$x$
$\tau = \overleftarrow{v}_{u,n}(V, x)$	—	—	$\sqrt{V}$		—	—
$V = \overrightarrow{v}_{u,n}(\tau, x)$	—	—	$\tau^2$		—	—
effort (core mins, $U = 5$ )	46.3	6.7	9.3	2.5	2.4	0.3
effort (core mins, $U = 10$ )	77.7	11.7	15.4	5.1	4.7	0.6
effort (core mins, $U = 20$ )	143.8	21.8	28.7	10.9	9.4	1.1
effort (core mins, $U = 40$ )	276.8	42.5	57.8	25.8	19.0	2.0
effort (core mins, $U = 80$ )	539.1	83.3	186.6	84.0	37.2	4.0

Table S-4: Algorithmic settings for the Lorenz '96 numerical example. Computational effort is measured in core minutes for running one filter, corresponding to a point on Figure Figure S-5. The time taken for computing a single point using the parallel BIF, ASIF and ASIF-IR implementations is the effort divided by the number of cores, here 30. The time taken for computing a single point using the serial GIRF, PF and EnKF implementations is equal to the effort in core minutes.

## S10 A memory-efficient representation of ASIF

The ASIF pseudocode in the main text emphasizes the logical structure of the mathematical quantities computed, rather than describing a specific implementation. Arguably, an algorithm should specify not only what is to be computed, but also details of what variables should be created and saved to carry out these computations efficiently, and how computations and storage are shared across multiple locations when the algorithm is parallelized. We use the term algorithm to denote a higher level description of the quantities to be calculated and we will say that alternative pseudocodes arriving at the same quantities are representations of the algorithm. Here, we present an alternative representations of ASIF which we call ASIF<sub>2</sub>, and we refer to the representation in the main text as ASIF<sub>1</sub>. The most concrete form of an algorithm is the actual computer code implementing the algorithm in a programming language. The implementation of ASIF in `spatPomp`, used for numerical results in this paper, uses an embarrassingly parallel approach based on the representation ASIF<sub>1</sub>. This strategy facilitates robust and simple parallelization, and is appropriate when memory constraints are not limiting. To develop ASIF<sub>2</sub>, we set up notation similar to that used for the mathematical theory. Let

$$\gamma_{u,n,i,k} = \frac{1}{J} \sum_{j=1}^J \prod_{\tilde{u}: (\tilde{u}, n-k) \in B_{u,n}} w_{\tilde{u}, n-k, i, j}^M \quad (\text{S58})$$

Also, let

$$\gamma_{u,n,i,0}^+ = \frac{1}{J} \sum_{j=1}^J \prod_{(\tilde{u}, n) \in B_{u,n}^+} w_{\tilde{u}, n, i, j}^M \quad (\text{S59})$$

Now set  $K$  to be the largest value of  $k$  for which  $B_{u,n}^{[n-k]}$  is nontrivial for some  $(u, n)$ , i.e.,  $K$  is the largest temporal lag in any neighborhood. With this notation, we can write (S32) as

$$\begin{aligned} \gamma_{B_{u,n}}^{MC,i} &= \prod_{k=0}^K \gamma_{u,n,i,k} \\ \gamma_{B_{u,n}^+}^{MC,i} &= \gamma_{u,n,i,0}^+ \prod_{k=1}^K \gamma_{u,n,i,k} \end{aligned}$$

This motivates the following representation of ASIF.

---

**ASIF<sub>2</sub>. Adapted simulation island filter, representation 2.**


---

Initialize adapted simulation:  $\mathbf{X}_{0,i}^A \sim f_{\mathbf{X}_0}(\mathbf{x}_0)$   
For  $n$  in  $1:N$   
Proposals:  $\mathbf{X}_{n,i,j}^P \sim f_{\mathbf{X}_n|X_{1:U,n-1}}(\mathbf{x}_n | \mathbf{X}_{n-1,i}^A)$   
Measurement weights:  $w_{u,n,i,j}^M = f_{Y_{u,n}|X_{u,n}}(y_{u,n}^* | X_{u,n,i,j}^P)$   
Adapted resampling weights:  $w_{n,i,j}^A = \prod_{u=1}^U w_{u,n,i,j}^M$   
Resampling:  $\mathbb{P}[r(i) = a] = w_{n,i,a}^A \left( \sum_{k=1}^J w_{n,i,k}^A \right)^{-1}$   
 $\mathbf{X}_{n,i}^A = \mathbf{X}_{n,i,r(i)}^P$   
Compute  $\gamma_{u,n+k,i,k}$  for  $k$  in  $0:K$ ,  
Compute  $\gamma_{u,n,i,0}^+$   
End for  
 $\ell_{u,n}^{\text{MC}} = \log \left( \frac{\sum_{i=1}^{\mathcal{I}} \gamma_{u,n,i,0}^+ \prod_{k=1}^K \gamma_{u,n,i,k}}{\sum_{i=1}^{\mathcal{I}} \prod_{k=0}^K \gamma_{u,n,i,k}} \right)$

---

It is clearer from the ASIF<sub>2</sub> representation than from the ASIF<sub>1</sub> representation that we do not have to save every individual particle and its weight  $w_{u,n,i,j}^M$  after the quantities  $\mathbf{X}_{n,i}^A$ ,  $\gamma_{u,n+k,i,k}$  and  $\gamma_{u,n,i,0}^+$  have been computed. ASIF<sub>2</sub> has an embarrassingly parallel implementation, since the islands do not need to interact until they are combined to compute  $\ell_{u,n}^{\text{MC}}$ . An embarrassingly parallel implementation therefore requires  $O(U(KN+J))$  memory for each island, and  $O(UNZK)$  memory when the results from each island are collected together.

By using additional communication, for example when the implementation is designed for a single core or multiple cores with shared memory, it is possible to further reduce the memory requirement. At time  $n$ , we need to save only  $\mathbf{X}_{n,i}^A$  and  $\gamma_{u,n-K:n+K,i,k}$  to compute  $\ell_{u,n}^{\text{MC}}$  and all subsequent quantities. Computing  $\mathbf{X}_{n,i}^A$  requires  $O(UJ)$  storage. Therefore, ASIF can be implemented with memory requirement  $O(U(K\mathcal{I} + J))$ , independent of  $N$ .

## Supplementary References

- Ades, M. and Van Leeuwen, P. J. (2015). The equivalent-weights particle filter in a high-dimensional system, *Quarterly Journal of the Royal Meteorological Society* **141**(687): 484–503.
- Evensen, G. and van Leeuwen, P. J. (1996). Assimilation of geostat altimeter data for the Agulhas Current using the ensemble Kalman filter with a quasigeostrophic model, *Monthly Weather Review* **124**: 58–96.
- Liu, J. S. (2001). *Monte Carlo Strategies in Scientific Computing*, Springer, New York.
- Lorenz, E. N. (1996). Predictability: A problem partly solved, *Proceedings of the Seminar on Predictability* **1**: 1–18.
- Park, J. and Ionides, E. L. (2019). Inference on high-dimensional implicit dynamic models using a guided intermediate resampling filter, *Arxiv:1708.08543v3*.